

**Zone of Representation of PM_{2.5} Chemical Composition during the California
Regional PM₁₀/PM_{2.5} Air Quality Study (CRPAQS)**

J. C. Chow, L.-W. A. Chen , J. G. Watson, D.H. Lowenthal
Division of Atmospheric Sciences, Desert Research Institute, Reno, NV 89512

K. Magliano
California Air Resources Board, Sacramento, CA 95814

D. Lehrman
Technical and Business Systems, Santa Rosa, CA 95404

Submitted to

Journal of Geophysical Research

June 17, 2005

ABSTRACT

The 14-month Central California PM₁₀/PM_{2.5} Air Quality Study (CRPAQS) acquired speciated PM_{2.5} measurements at 38 sites representative of urban, boundary, and rural environments in the San Joaquin Valley (SJV) air basin. These observations are used to determine the spatial variability of PM_{2.5}, ammonium nitrate (NH₄NO₃), and carbonaceous material on annual, seasonal, and episodic time scales, and to understand the mechanism for the formation of severe pollution episodes. The PM_{2.5} and NH₄NO₃ concentration decreased rapidly with altitude, confirming the influence of topography on the ventilation and transport of pollutants. Elevated PM_{2.5} from November to January contributed to 50 – 75% of the annual averages, but the contributions from NH₄NO₃ and organic matter differ substantively between urban and rural areas. Winter meteorology and intensive residential wood combustion are likely key factors for the winter-nonwinter and urban-rural contrast. Intensive operating periods during CRPAQS reveal the role of upper-layer currents on the valleywide transport of NH₄NO₃. Site zone of representations with respect to different species are evaluated to further improve the monitoring network.

Index Terms: Atmospheric composition and structure, Middle atmosphere: composition and chemistry, Middle atmosphere: constituent transport and chemistry, Pollution: urban and regional, Synoptic-scale meteorology

Keywords: Fresno Super Site, San Joaquin Valley Air Basin, PM Spatial Distribution

1. Introduction

The spatial and temporal distributions of particulate mass (PM) and chemical constituents are essential for understanding source-receptor relationships as well as chemical, physical, and meteorological processes that result in elevated concentrations in central California. There is much variability throughout central California and its major geographical feature, the San Joaquin Valley (SJV). Variability in emissions, meteorology, and terrain are expected to result in substantial differences in particulate concentrations and compositions.

The SJV air basin is bordered on the west by the coastal mountain range and on the east by the Sierra Nevada range. These ranges converge at the Tehachapi Mountains at the southern end of the basin, ~ 200 km south of Fresno (the largest population center ~150 km to both the north and south of the basin). Weather changes with season throughout the year. Spring often experiences small frontal passages with low moisture content resulting in high winds. Summer meteorology is driven by heating over the Mojave desert, which creates a thermal low pressure system and a large pressure gradient between the coast and the desert. Fall and winter are influenced by the Great Basin High, with prolonged periods of slow air movement and limited vertical mixing. Morning mixing depths and ventilation are low in all seasons and remain low throughout the day during winter. Relative humidity (RH) is highest in the winter, with lows in the summer and fall.

Central California emission source categories include: 1) small- to medium-sized point sources (e.g., power stations, natural gas boilers, steam generators, incinerators, and cement plants); 2) area sources (e.g., wind-blown dust, petroleum extraction operations, cooking, wildfires, and residential wood combustion [RWC]); 3) mobile sources (e.g., cars, trucks, off-road heavy equipment, trains, and aircraft); 4) agricultural and ranching activities (e.g., tilling, fertilizers, herbicides, and livestock); and 5) biogenic sources (e.g., nitrogen oxides [NO_x] from biological activity in soils and hydrocarbon [HC] emissions from plants). Agriculture is the main industry in the central valley, with cotton, alfalfa, corn, safflower, grapes, and tomatoes being the major crops. Cattle feedlots, dairies, chickens, and turkeys constitute most of the animal husbandry in the region and are a major source of ammonia (NH₃) emission.

The SJV contains one of the largest PM_{2.5} and PM₁₀ (particles with aerodynamic diameters less than 2.5 and 10 micrometers [μm], respectively) non-attainment areas in the United States. Elevated PM concentrations frequently occur in winter. Past studies (Chow et al., 1992, 1993, 1996, 1998) have shown that wintertime PM concentrations were primarily in the PM_{2.5} size fraction. Chemical mass balance receptor models (Magliano et al., 1999; Schauer and Cass, 2000) attributed winter PM episodes in urban areas to RWC emission, motor vehicle

exhaust, and secondary ammonium nitrate (NH_4NO_3). NH_4NO_3 generally accounts for 30% to 60% of $\text{PM}_{2.5}$ (Magliano et al., 1998a, 1998b, 1999; Chow and Watson, 2002) and nearly half of PM_{10} (Chow et al., 1992, 1996, 1999). Vehicular exhaust and RWC emission are mostly $\text{PM}_{2.5}$ in the form of organics or organic matter ($\text{OM} = \text{OC} \times 1.4$) and elemental carbon (EC).

Watson et al. (1998) developed a conceptual model that described the interaction between gaseous precursors and primary particle emissions from urban and non-urban areas under the stagnant, moist, and foggy conditions that often present in the SJV during winter, and how the transport and interactions leads to the formation of severe PM episodes. A better spatial resolution of distributions of $\text{PM}_{2.5}$ and its major components, particularly NH_4NO_3 and OM, on different temporal scales are essential to confirm this conceptual model.

The California Regional $\text{PM}_{10}/\text{PM}_{2.5}$ Air Quality Study (CRPAQS) was dedicated to understand the causes of PM pollution in central California and to evaluate means to reduce them (Watson et al., 1998). To examine the variability in this region, CRPAQS set up a $\text{PM}_{2.5}$ network consisting of 38 sites (Figure 1) that acquired ambient measurements for continuous 14 months. This network covered the SJV and surrounding air basins (i.e., San Francisco Bay, Sacramento Valley, Mountain Counties, Great Basin Valleys, and Mohave Desert,), containing urban, suburban, regional, transport, and rural background environments. The objectives of this paper are to: 1) assess the ambient $\text{PM}_{2.5}$ concentrations; 2) examine $\text{PM}_{2.5}$ mass closure and its seasonal dependence; 3) resolve spatial variability of $\text{PM}_{2.5}$ mass and chemical composition on different temporal scales; and 4) evaluate the zone of representation/influence of individual sampling sites and its implication on air quality monitoring and management.

2. Ambient Network

The CRPAQS ambient network covers a region ~600 km long by 200 km wide (Figure 1). The sampling program spanned a 14-month period between 2 December 1999 and 3 February 2001, including an annual program between 1 February 2000 and 31 January 2001 and winter intensive operating periods (IOPs) for 13-15 forecasted episode days between 15 December 2000

and 3 February 2001. The annual program included daily 24-hr sampling at three anchor sites - Fresno Supersite (FSF, part of the U.S. Environmental Protection Agency [EPA] Supersite program), Bakersfield (BAC) and Angiola (ANGI); and every sixth day 24-hr sampling at 35 satellite sites (Table 1). Winter IOPs included five times/day 3-8 hour samples for 15 days at the five anchor sites - FSF, ANGI, BAC, Bethel Island (BTI), and Sierra Foothills (SNFH), and daily 24-hour sampling for 13 days at 25 satellite sites.

FSF and BAC represent two major urban centers in the SJV. The ANGI site is located between the two urban centers to represent a regional transport environment. BTI and SNFH represent the inter-basin gradient and transport boundary conditions and were operated during the winter IOPs. BTI is located at the northwest corner of SJV and ~ 50 km east of San Francisco, CA. SNFH (589 m above mean sea level [MSL]) is roughly parallel to FSF, situated at the fast-ascending slope of the western Sierra Nevada. Depending on the land use and surrounding environs, the satellite sites are categorized into eight site-types (Table 1), including 18 community exposure sites, 11 emissions source dominated sites, 9 visibility sites, 11 intrabasin gradient sites, 2 vertical gradient sites, 1 intrabasin transport site, 6 inter-basin transport sites, and 7 boundary/background sites.

At each of the anchor sites, a Desert Research Institute (DRI, Reno, NV, USA) sequential filter sampler (SFS) (Chow et al., 1994, 1996; Chen et al., 2002) was installed. Each SFS contains two sampling channels (20 liters per minute [L/min]) downstream of a PM_{2.5} size-selective inlet (Model 240 cyclone, Bendix/Sensidyne, Clearwater, FL, USA), operated at 113 L/min, and an anodized-aluminum-coated nitric acid (HNO₃) denuder. The first channel contains a Teflon-membrane filter (#R2PJ047, Pall Corporation, Putnam, CT, USA) followed by a citric acid impregnated cellulose-fiber backup filter (31ET, Whatman, Brentford, Middlesex, UK) (i.e., FTC filter pack). The Teflon-membrane filter is used for: 1) determination of PM_{2.5} mass by gravimetry (for filter equilibrated at 21 ± 1.5 °C and 35 ± 5% RH in a controlled laboratory environment); 2) filter light transmission (b_{abs}) by densitometer; and 3) ~ 40 elements by X-ray fluorescence (XRF, Watson et al., 1998). The backup cellulose-fiber filter is to detect

ammonia (NH_3) as ammonium (NH_4^+) by automated colorimetry (AC). The parallel channel contained a quartz-fiber filter (#2500QAT-UP, Pall Corporation, Putnam, CT, USA) followed by a sodium chloride-impregnated cellulose-fiber backup filter (31ET, Whatman, Brentford, Middlesex, UK) (i.e., FQN filter pack). The quartz-fiber filter is for determining: 1) organic carbon (OC) and EC by thermal-optical reflectance (TOR) method following interagency monitoring of protected visual environments (IMPROVE) protocols (Chow et al., 1993, 2001, 2004; Chen et al., 2004; Watson et al., 1994), 2) water-soluble sodium (Na^+) and potassium (K^+) by atomic absorption spectrometry (AAS); 3) NH_4^+ by AC; and 4) chloride (Cl^-), NO_3^- , and sulfate (SO_4^{2-}) by ion chromatography (IC). The backup cellulose-fiber filter collects NO_3^- volatilized from the quartz-fiber filter to minimize a negative bias in NO_3^- measurements (Zhang and McMurray, 1992; Herring and Cass, 1999; Chow et al., 2005). In this paper, NO_3^- represents the sum of non-volatilized NO_3^- from the front filter and volatilized NO_3^- from the backup filters. Two sequential gas samplers (SGSs) (Chow et al., 1996; Chen et al., 2002) were also installed at the five anchor sites during winter IOPs for quantifying gaseous HNO_3 and NH_3 using the denuder difference method.

Battery-powered MiniVol samplers (AirMetrics, Springfield, OR, USA) are deployed at the satellite sites, equipped with tandem PM_{10} and $\text{PM}_{2.5}$ impactors operated at 5 L/min. Filter-pack assembly for the $\text{PM}_{2.5}$ satellite sites follows the same FTC and FQN configurations of those at the anchor sites, with mass, elements, and NH_3 acquired at all 35 sites; Carbon, ions, and volatilized NO_3^- acquired at 29 sites as noted in Table 1. $\text{PM}_{2.5}$ MiniVol samplers are shown to yield mass concentration equivalent to $\text{PM}_{2.5}$ Federal Reference Method (FRM) compliance samplers (Baldauf et al., 2001, Chow et al., 2005). Occasional malfunctions of battery and pump resulted in missing data. Each satellite site typically reports more than 80% valid mass measurements over the study period (Table 2), except for the feedlot or dairy (FEDL; 62%), Edwards (EDW; 77%), and Bakersfield RWC dominated (BRES; 66%) sites. Since the missing data were random in time, they are not expected to bias the annual averages.

Uncertainty was determined for each measurement based on flow rate performance test and replicate analysis. For mass, NO_3^- , NH_4^+ , and total carbon ($\text{TC}=\text{OC}+\text{EC}$), the uncertainty is typically within $\pm 10\%$ for a measured value which exceeds ten times minimum detection level (MDL). Measured NO_3^- are compared to NH_4^+ as part of the data validation. The high correlation ($R^2 \sim 0.99$) between the two species and nearly 1:1 molar ratio indicate the dominant form of NH_4^+ in the atmosphere as NH_4NO_3 . Only $\sim 9\%$ of NH_4^+ is associated with other anions, likely SO_4^{2-} and Cl^- . Hereafter the concentration of NH_4NO_3 is estimated by $1.29 \times [\text{NO}_3^-]$.

3. Spatial Variations of $\text{PM}_{2.5}$ Mass and Seasonal Contributions

Fourteen of the 38 CRPAQS sites exceeded the U.S. annual $\text{PM}_{2.5}$ National Ambient Air Quality Standard (NAAQS) of $15 \mu\text{g}/\text{m}^3$ (Table 2). Widespread exceedances in the southern part of SJV occurred in both urban areas of FSF ($23.3 \mu\text{g}/\text{m}^3$), Visalia (VCS: $21.7 \mu\text{g}/\text{m}^3$), and BAC ($26.0 \mu\text{g}/\text{m}^3$) and relatively rural areas, such as ANGI ($18.7 \mu\text{g}/\text{m}^3$). Although these annual averages are based on averages of the four calendar quarters (U.S. EPA, 1997), Table 2 shows that they differ from every-sixth-day arithmetic means of the annual or 14-month program by $<10\%$, except at BRES. This corroborates the limited impact of missing data on the annual averages. Hereafter, the every-sixth-day average is used.

The $\text{PM}_{2.5}$ concentration decreases rapidly towards the elevated valley boundary (Figure 2a). Three sites in Bakersfield (RWC dominated BRES site, urban BAC site, and inter-basin gradient Edison [EDI] site, all ~ 118 m MSL) reported consistent high $\text{PM}_{2.5}$ of $24 - 28 \mu\text{g}/\text{m}^3$ in annual average, despite the fact that each site represents different microenvironments. Tehachapi (TEH2), an inter-basin transport site, located < 50 km to the southeast of EDI but elevated at 1229 m MSL, recorded an annual $\text{PM}_{2.5}$ of $7.3 \mu\text{g}/\text{m}^3$. The $\text{PM}_{2.5}$ concentration decreases further at the Mohave Desert, EDW (724 m MSL) and Mojave-Pool (MOP; 832 m MSL) sites, averaging only $4.3 - 5.4 \mu\text{g}/\text{m}^3$ annually. Similarly, annual $\text{PM}_{2.5}$ decreases from $23.7 \mu\text{g}/\text{m}^3$ at FSF, to $20.8 \mu\text{g}/\text{m}^3$ at Clovis (CLO; 108 m MSL, a suburban site ~ 10 km east of Fresno), and to $8.5 \mu\text{g}/\text{m}^3$ at SNFH (589 m MSL, 33 km east of CLO). This reflects the influence of topography

on the PM_{2.5} distribution. North of Fresno, the PM_{2.5} concentration is relatively low even at the urban centers of Sacramento (S13, 11.1 µg/m³) and San Francisco (SFA, 9.2 µg/m³), with the highest concentration of 17.3 µg/m³ observed at Modesto (M14).

The strong vertical gradient of PM_{2.5} is consistent with the dominant local emissions and limited inter-state transport. The Sierra Nevada and coastal mountains form a ceiling that prevents precursor gases and particles released in the SJV from quick dispersion. To some extent the valley is isolated from the influences of distant sources, especially in the southern SJV due to a deeper concave structure. The SJV floor generally increases in elevation from north to south until Fresno, then elevation decreases. The five most northeastern sites in this network, located at Bodega Bay (BODG), BTI, SFA, S13 and Stockton (SOH), all have elevations less than 10 m MSL. There could be more frequent exchanges between valley air and cleaner marine air at these sites, leading to the lower PM_{2.5} observed in the northern valley.

Sources of NH₃ include the decay of plant material and animal waste, especially from commercial dairy and feedlots on account of their large animal populations. There are also minor NH₃ emissions from fertilizer industry and gasoline vehicles. Annual NH₃ concentrations up to 25 µg/m³ occurred in a broad rural area containing ANGI, Pixly Wildlife Refuge (PIXL), Corcoran-Patterson (COP), and Visalia (VCS) (Figure 2b). A secondary high of ~ 20 µg/m³ was measured at Southwest Chowchilla (SWC). At Fresno, it was generally below 12 µg/m³ (note: FEDL is exceptional but contains ~ 40% missing data). NH₃ is one of the most important PM precursors. NH₄NO₃ is formed through the reaction of NH₃ with NO_x released primarily from urban areas. This PM formation mechanism must involve the mixing of urban and rural airs.

Between mid-February 2000 and late October 2000, 24-hr PM_{2.5} concentrations at FSF were generally within 15 µg/m³ (Figure 3). PM_{2.5} concentrations frequently exceeded 15 µg/m³ from November to January, and reached the maximum of 148.3 µg/m³ on 1 January 2001. A similar temporal pattern is found at BAC, which often reported higher PM_{2.5} concentrations. Schauer and Cass (2000) suggested that RWC contributes to 14% – 63% of PM_{2.5} at Fresno and Bakersfield, mostly in the form of organic matter during winter. RWC alone is unlikely to

explain the increase of PM_{2.5} by one order of magnitude from summer to winter. The meteorological effect on the ventilation of pollutants and formation of secondary aerosol is critical in this scenario.

The regional transport ANGI site, which is proximate to the Tulare Lake and surrounded with farm fields and sparse residents, experienced wintertime PM_{2.5} episodes with similar intensity to those in FSF and BAC (Figure 3). Though winter highs also appeared at the other two inter-basin anchor sites (BTI and SNFH), they are much less pronounced. BODG in Figure 3 represents the northern boundary/background site, while the ACP (373 m MSL) and TEH2 (1229 m MSL) sites represent the eastern and southern intra- and inter-basin transport sites of the SJV. No appreciable seasonal variations were observed at these transport and boundary sites, especially at BODG and TEH2. This is consistent with the conceptual model; there is very little influence of synoptic-scale transport on background PM_{2.5} level.

The patterns of temporal variations in Figure 3 reflected limited differences between spring (March to May) and summer (June to August) PM_{2.5} averages (Table 2). To the north of FSF, the highest spring PM_{2.5} occurred at BODG (10.5 µg/m³), similar to those at FSF (11.2 µg/m³) and the Fresno residential site (FRES: 9.0 µg/m³). Urban-rural contrast was at a minimum in the northern SJV from spring to summer. Three sites within the Bakersfield urban area (BAC, BRES, and EDI) recorded a wide range of PM_{2.5} (7.9 to 19.8 µg/m³) in spring, likely due to dominant effects of the micro-environment related to site characteristics. The source-dominated Fresno feedlot (FEDL) reported an elevated PM_{2.5} level (25.3 to 27.8 µg/m³) during summer and fall, reflecting intensive farming activities; these elevated PM_{2.5} concentrations reached the maximum of 38.6 µg/m³ in winter. The two urban (FSF and BAC) and regional transport ANGI sites reported three- to six-fold increase in PM_{2.5} from spring/summer to winter. The CRPAQS annual program is further divided into high (C_{high}; 1 January 2000 to 31 January 2001) and low (C_{low}; 1 February 2000 to 31 October 2000) PM_{2.5} periods for comparison as shown in Table 2. PM_{2.5} exceeded the annual NAAQS of 15 µg/m³ in Bakersfield (BAC, EDI) even during the low period. The maximum C_{low}, however, occurred at the FEDL site (23.7

$\mu\text{g}/\text{m}^3$). The impact of the high period to annual averages (i.e., F_{high}), defined in Table 2, ranged from 13% at China Lake (CHL) to 72% at M14. C_{high} in general contributes to > 50% of annual $\text{PM}_{2.5}$ loading inside the valley, 55% at the BAC and 63% at the FSF urban centers. F_{high} is < 25% only at three sites: CHL (10%), MOP (17%), and Olancha (OLW; 15%), all of which are located in the Mohave Desert or Great Basin Valleys. The slightly higher C_{low} than C_{high} at these elevated rural sites suggests the impact from long-range transport in spring and summer (Green, 1999).

4. $\text{PM}_{2.5}$ Chemical Compositions

Previous studies conducted in the SJV (e.g., Chow 1996; 1999) consent that $\text{PM}_{2.5}$ mostly consists of NH_4NO_3 and organics, while PM_{10} mainly consists of crustal material (CM). Table 2 presents the annual averages of the five main $\text{PM}_{2.5}$ components (i.e., NH_4NO_3 , $(\text{NH}_4)_2\text{SO}_4$, OM, EC, and CM), as well as the reconstructed $\text{PM}_{2.5}$ mass. Though overall the reconstructed mass explains 92% of the $\text{PM}_{2.5}$ gravimetric mass (i.e., $R^2 = 0.92$), appreciable negative or positive biases are found at individual sites (see mass closure in Table 2). The negative bias is due to uncounted species, such as water (H_2O). The positive bias are common for rural sites where $\text{PM}_{2.5}$ concentration are relatively low; it most likely results from organic sampling artifact, i.e., the adsorption of ambient volatile organic compounds (VOCs) onto quartz-fiber filters (Turpin et al., 1994; Chow and Watson; 2002; Chow et al., 2005). This artifact may partially be compensated by the evaporation of particulate OM from the filters (Zhang and McMurray, 1987; Chen et al., 2002; Subramanian et al., 2004). OM/OC ratios higher than 1.4 were reported (Turpin et al., 2001; El-Zemin et al., 2005), and this further complicates the quantification of OM mass. Nevertheless, NH_4NO_3 and OM are dominant fractions in $\text{PM}_{2.5}$, accounting for >77% of the annual $\text{PM}_{2.5}$ mass in urban areas.

To visualize the spatial variability, C_{low} and C_{high} were calculated for $\text{PM}_{2.5}$ mass and major chemical components for each site and for the entire study domain using a triangle-based cubic interpolation algorithm (Barber et al., 1996; Sandwell, 1987). Sites with more than 30%

missing data were excluded from the calculation. Four geographic cross-sections (i.e., A, B, C, and D) are selected (defined in Figure 2b), along which concentrations of chemical components are compared with PM_{2.5} mass (Figure 4). These cross-sections intersect each other at Fresno (FSF) and have covered major geographical features of the SJV. During C_{low}, urban areas appeared to experience slightly high PM_{2.5} relative to rural areas. A nearly-uniform OM distribution is observed along the cross-section C that stretches between the Sierra Nevada and the coastal mountains (Longitude 119.3 – 120.5°W). NH₄NO₃ is generally < 7 µg/m³ throughout the valley floor, decreasing to ~ 2 µg/m³ at the elevated mountain sites of ACP, CHL, and SNFH. A majority of NO₃⁻ (> 80%) was found on the front quartz-fiber filter, except at BAC (cross-section B) where more than 50% of NO₃⁻ was found on the backup cellulose-fiber filter. (NH₄)₂SO₄ and CM are relatively minor components of PM_{2.5}.

During C_{high} from late fall to winter, NH₄NO₃ concentration increases by several folds in the southern SJV air basin, with the highest level of ~ 30 µg/m³ observed at BAC. Elevated NH₄NO₃ were not limited to urban areas. A rural site in central Fresno county, (HELM; 55 m above MSL; in cross-section C), ~ 41 km to the west of FSF, reported a NH₄NO₃ concentration of ~ 17.1 µg/m³, close to those in the Fresno area (19 – 22 µg/m³). However, NH₄NO₃ concentration decreased rapidly with altitude. The elevated MOP site (832 m above MSL) reported 1.1 and 1.3 µg/m³ NH₄NO₃ during C_{low} and C_{high}, respectively. A similar level of volatilized NO₃⁻ was found on the backup filter during C_{high} but accounted for a lower fraction of total particulate NO₃⁻. Figure 4 demonstrates that widespread NH₄NO₃ is the key factor resulting in basin-wide PM_{2.5} episodes.

NO₃⁻ ions form from their gaseous precursor (NO_x) mostly in the aqueous phase, where they react with NH₄⁺ ions to form NH₄NO₃. The cold and humid weather during winter do favor NH₄NO_{3(aq)} over gaseous HNO₃ and NH₃ (Seinfeld and Pandis, 1998; Takahama et al., 2004; Moya et al., 2001). The seasonal cycle of the NH_{3(g)}/NH₄⁺_(aq) ratio at FSF (Figure 5) confirms the shift of equilibrium towards NH_{3(g)} in the spring-fall period. Surface wind speeds in the SJV are very low, often <1 m/sec during winter, with variable surface wind directions. Surface

transport distances estimated from these wind speeds are insufficient to account for the mixing of non-urban NH₃ emissions with urban NO_x emissions for the formation of widespread NH₄NO₃ (Smith and Lehrman, 1994). Regional transport/mixing is likely accomplished by upper-layer (> 200 m) current. The higher NH₄NO₃ concentration in the southern SJV is also consistent with higher NH₃ concentrations.

Contrasting to NH₄NO₃, there were no appreciable increases of OM at rural sites, such as HELM, BTI, and ANGI (Figure 4) during C_{high}. While NH₄NO₃ increased from 3.5 µg/m³ (C_{low}) to 17.1 µg/m³ (C_{high}) at HELM, the OM concentration remained between 4.5 and 5.5 µg/m³. OM was lower during winter at the elevated rural CHL site. OM levels of 10 µg/m³ or higher were generally confined within a few urban zones: M14, VCS, FSF, and BAC, and this exacerbated urban PM pollution. The accumulation of primary pollutants is enhanced under a more stable and stagnant winter boundary layer. As part of the CRPAQS, Rinehart et al. (2005) conducted organic speciation for 20 sites in the SJV, and reported a high percentage of levoglucosan in Fresno, a marker for RWC emission (Mochida and Kawamura, 2004; Fine et al., 2002; Simoneit, 2002; Simoneit et al., 1999). Residential use of wood fuel in winter that clustered in urban areas contributed more to the elevated OM than motor vehicle emissions. EC generally tracks OM but the OM/EC ratio is higher at urban sites where excessive OM is produced. Crustal material is low, especially during C_{high}.

Summed mass of NH₄NO₃, OM, and EC exceeds the gravimetric PM_{2.5} mass during C_{low} (Figure 4). The bias would have been even larger if (NH₄)₂SO₄ and CM are included or a higher OM/OC ratio (> 1.4) is used. It should be noted that the positive artifact due to organic vapor adsorption is not corrected in this study. Previous studies (e.g., Chow and Watson, 2002; Chow et al., 1996, 2005) reported equal or higher OC on the backup filter (surrogate for organic vapor adsorption) of a quartz-quartz tandem filter pack in summer than in winter. Providing that particulate OC is, in general, lower in summer, this artifact becomes more significant in terms of mass percentage. For C_{high}, NH₄NO₃, OM, and EC explain the PM_{2.5} mass sufficiently in rural areas, but not in urban areas despite the positive OM sampling artifact (Figure 4). Less than a

half of the ~ 20% residual mass at FSF and VCS can be attributed to $(\text{NH}_4)_2\text{SO}_4$, CM, and sea salt. H_2O could also contribute to the unidentified mass (Malm et al. 1994; Andrews, 2000; Rees et al., 2004; Khlystov et al., 2005). The Teflon-membrane filters were weighed at $35\pm 5\%$ RH, but H_2O associated with hygroscopic NH_4NO_3 and $(\text{NH}_4)_2\text{SO}_4$ crystals may not be completely evaporated. The amount of residue H_2O should be proportional to the NH_4NO_3 concentration.

5. Winter $\text{PM}_{2.5}$ Episodes

The winter IOPs (IOP_1: 15 December 2000 to 18 December 2000; IOP_2: 26 December 2000 to 28 December 2000; IOP_3: 4 January 2001 to 7 January 2001; and IOP_4: 31 January 2001 to 3 February 2001) were forecasted based on the boundary layer stability, considering wind speed, mixing height, and RH; they agreed closely in time with the elevated $\text{PM}_{2.5}$ concentration in the valley (Figure 3). At the five anchor sites, each sampling day is segregated into five time-integrated measurements (0000 – 0500, 0500 – 1000, 1000 – 1300, 1300 – 1600, and 1600 – 2400 Pacific standard time [PST]). Daily $\text{PM}_{2.5}$ concentrations were calculated by time-weighted averages to be compared with 24-hr measurements at the satellite sites.

Spatial trends on each sampling day between 15 December 2000 and 3 February 2001, including the four IOPs, were calculated with the cubic-spline algorithm considering all concurrent 24-hr measurements. Figure 6 presents the concentrations of $\text{PM}_{2.5}$ mass, NH_4NO_3 , and OM along the geographic cross-section D constructed to represent the valley's primary axis (defined in Figure 2b). No apparent contrasts on $\text{PM}_{2.5}$ or chemical components were found during IOP_1. NH_4NO_3 started to build up during IOP_2 (26 December 2000) in the southern SJV and appeared to persist through early January 2001. Elevated OM ($> 40 \mu\text{g}/\text{m}^3$) was also observed around urban centers, including M14, FSF, and BAC.

IOP_3 captured a major $\text{PM}_{2.5}$ episode driven by NH_3NO_3 . On 4 January 2001, NH_3NO_3 in the southern SJV accumulated up to $75 \mu\text{g}/\text{m}^3$, and by 5 January 2001, this plume blanketed a broad region between FSF and BAC. The peak concentration of this episode, $\sim 100 \mu\text{g}/\text{m}^3$ NH_4NO_3 , was reached at ANGI and PIXL (~ 15 km south of ANGI) on 6 January 2001.

Meanwhile, the plume extended to the north of FSF; for the first time in the winter, M14 recorded a NH_4NO_3 concentration higher than $60 \mu\text{g}/\text{m}^3$. While NH_4NO_3 gradually dissipated in the southern SJV after 6 January 2001, BTI, a northern boundary site, reported NH_4NO_3 of $40 \mu\text{g}/\text{m}^3$ on 7 January 2001, compared with $\sim 50 \mu\text{g}/\text{m}^3$ at FSF. The laden NH_4NO_3 peak moving northward from the south, suggesting a regional transport. Based on 24-hr back trajectories, Chow et al. (1999) estimated the maximum influence of emissions mixed aloft are 519 km and 1266 km at the FSF and BAC sites, respectively. Winds aloft (> 200 m AGL) are sufficient to transport pollutants aloft throughout the SJV in 24 hours, even though surface wind speeds are low and transport distances are small.

Low surface wind speeds, however, prevent ventilation of primary $\text{PM}_{2.5}$ near their sources. The primary $\text{PM}_{2.5}$ is mostly OM and EC from RWC or motor vehicle exhaust and CM from wind-blown dust. IOP_2 and IOP_3 feature a mean surface wind speed of 1 – 2 m/sec at FSF, and a substantial accumulation of OM was observed around this site. High OM levels also appeared at M14 and BAC. In general, OM tracked NH_4NO_3 on a 2-3-day time scale, consistent with synoptic scale meteorology. From IOP_2 through IOP_3, the SJV was between a persistent high-pressure ridge over the Great Basin and a surface low just off the southern California coast. Back-trajectory analysis reveals a calm surface layer and a weak southeasterly current aloft (100 – 500 m AGL). By 8 January 2001, the surface low advanced into the continent, resulting in precipitation on 9 January 2001 that ended the episode. Both OM and NH_4NO_3 reduced to lower than $10 \mu\text{g}/\text{m}^3$ till 13 January 2001 at BAC.

The final episode, IOP_4, is similar to IOP_2 with respect to synoptic meteorology and ambient $\text{PM}_{2.5}$ distribution. Valley-wide exceedance of the 24-hr $\text{PM}_{2.5}$ NAAQS of $65 \mu\text{g}/\text{m}^3$ at 26 sites were found during IOP_2, IOP_3, and IOP_4. In rural areas, these exceedances are mostly attributed to NH_4NO_3 , while towards urban areas there are increasing contributions from OM. This phenomenon also reflects the differences between secondary and primary aerosols.

6. Site Zone of Representation

The spatial extent that a monitoring site representing community exposure is essential for the design of an ambient air quality monitoring network. The optimal goal is to select sites that adequately capture the spatial variability while maintaining a minimum cost. CRPAQS consists of a regional-scale (100 – 1000 km) network according to the definition of the EPA (U.S. EPA, 1997), along with urban (4 – 100 km), neighborhood (0.5 – 4 km), middle- (0.1 – 0.5 km), and micro- (0.01 km – 0.1 km) scale sites. The median distance between two neighboring sites in the CRPAQS network is ~ 25 km, but they can be as close as a few kilometers in urban areas. For example, a vehicle exhaust dominated site (FREM) and a residential site (FRES) were set up ~1 km west and ~0.5 km east of the Fresno Supersite (FSF) in order to contrast different micro-environments (Watson and Chow, 2002).

The extent of representative zone for each site depends on the gradient of pollutant concentration around the site. Therefore, it could vary with temporal scale as well as species of concern. The first-order estimation involves calculating spatial distribution based on actual measurements (e.g., Figure 2) and finding the radius of a circular area in which the species concentration is no more than $\pm 20\%$ different from the center site. The criterion of 20% is chosen since it translates to a roughly 10% or less difference between the center site concentration and the average over the entire circular area, where 10% are in the same order of magnitude as the measurement uncertainty. This approach ensures that no extreme/singular points affects the zone of representation. Problems may arise for sites located on the boundary or corner of the study domain because concentrations outside the domain cannot be estimated. Table 3 summarizes the zone of representation of 26 non-boundary sites on the annual, seasonal, and episodic basis.

For annual $PM_{2.5}$, BTI and ANGI represent an area of 15 and 19 km in radius, respectively, greater than the urban sites of FSF and BAC (7 – 11 km). FSF represents very different zone radii for NH_4NO_3 (20 km) and OM (0.7 km), consistent with the strong gradient of OM concentration at the Supersite. The major contrast among the three sampling sites in Fresno

(FSF, FRES, FREM) and in its suburban site (CLO), therefore, would be caused by OM rather than NH_4NO_3 . Neighborhood-scale monitoring is necessary to resolve spatial variability of OM in an urban area. Despite being located in downtown Bakersfield, the BAC site appears to be representative of the entire city with respect to annual NH_4NO_3 and OM within 12 – 14 km of the radius. OM accounted for a minor fraction of $\text{PM}_{2.5}$ at the ANGI site, and therefore the $\text{PM}_{2.5}$ mass and NH_4NO_3 represented a similar zone. BTI is considered rural but influenced by nearby cities such as San Francisco (SFA), Sacramento (S-13), and Stockton (SOH). It represents a consistent zone (10 – 15 km) for $\text{PM}_{2.5}$ mass, NH_4NO_3 , and OM. SNFH is elevated (589 m above MSL), and its larger zone of representation for annual OM (14 km) than for NH_4NO_3 (5 km) is consistent with the rapid decrease of NH_4NO_3 concentration with increasing altitude.

The zones of representation during C_{high} are similar to those of the annual averages except at BAC, where the zones become much smaller for $\text{PM}_{2.5}$, NH_4NO_3 , and OM (< 5 km). The local emissions substantially lifted OM concentration near BAC in late fall and winter. For C_{low} , the zone of representation of OM at BAC is close to the background level in neighboring rural areas and this site can represent a zone up to 45 km in radius. In the boundary and transport sites, there is only a limited change of OM concentration at SNFH throughout the year; it represents a larger zone during C_{low} owing to a weaker gradient of OM concentration with altitude in summer. A sharp gradient in OM concentration is observed near BTI and ANGI for the low $\text{PM}_{2.5}$ period, leading to a smaller zone of representation of the two sites (7 – 9 km), which may have resulted from the inter-basin dispersion. Pollutants typically exhibit more spatial inhomogeneity on a short-term scale than a long-term scale. The zone of representation of FSF is reduced to < 2 km in radius, even for NH_4NO_3 , on an episodic day (7 January 2001), while corresponding zones of SNFH and ANGI sites all decrease from their annual averages. Ambient network design should consider both temporal and spatial scales, along with mass and chemical composition, in order to determine the site density for optimal results and costs.

7. Discussion and Conclusions

In comparison with other PM_{2.5} nonattainment areas (mostly on the mid-Atlantic coast or in the Midwest) in the U.S. (U.S. EPA, 2004), the problem of air quality degradation in the SJV is unique in nature. (NH₄)₂SO₄ is the major contributor to PM_{2.5} episodes in the eastern U.S. that often occur in summer when photochemistry is most active (Chen et al., 2003; Malm et al., 1994; 2004; Khlystov et al., 2005). The lack of mountain ridges allows (NH₄)₂SO₄ and carbonaceous aerosol to be transported thousands of kilometers downwind of their source regions. This results in elevated PM_{2.5} levels in a very broad downwind region. Twenty-four hour PM_{2.5} concentration seldom exceeds the PM_{2.5} NAAQS of 65 µg/m³ at any urban-scale sites even during summer episodes in the east, while it is common in central California. The source of sulfur dioxide (SO₂), a precursor of SO₄²⁻, is very limited in the SJV and in California. NH₃ released from agricultural activities alternatively reacts with NO₃⁻ to form NH₄NO₃. The topography, particularly mountains surrounding the valley, restricts the ventilation of pollutants that can accumulate to a very high level. The CRPAQS study shows a strong dependence of PM_{2.5} and NH₄NO₃ as a function of altitude. While widespread PM_{2.5} exceedances (up to 30 µg/m³) of annual NAAQS occurred in the southern SJV air basin, the PM_{2.5} concentration reduced to a near-background level immediately towards the mountainous boundary.

For most of the sites on the valley floor, 50 – 75% of annual PM_{2.5} can be attributed to a high PM_{2.5} period from November to January. In rural areas, the elevated PM_{2.5} is solely driven by NH₄NO₃. The temperature, RH, and stability of the valley boundary layer in winter are favorable for the formation of NH₄NO₃ from its precursors. Elevated OM exacerbates air quality mostly in urban areas. This is consistent with the extensive use of wood fuel for home heating in winter. Winter PM_{2.5} mass in urban areas cannot be fully explained by the five major components (i.e., NH₄NO₃, OM, EC, (NH₄)₂SO₄, and CM). H₂O may be an important part of the unidentified mass.

The IOPs during CRPAQS reveal the horizontal movement of pollution plumes during winter episodes. These observations corroborate previous investigations of the role of upper-layer

currents on the valleywide transport of NH_4NO_3 . However, CRPAQS produces $\text{PM}_{2.5}$ measurements of better spatial and temporal coverage than previous studies, and this provides a basis for conceptual and numerical models that attempt to link source emissions to ambient exposure. Most sites in the existing ambient network appear to represent either a urban- or a neighborhood-scale. This information are valuable for refining the air quality monitoring programs.

Acknowledgements

This work was supported by the California Regional $\text{PM}_{10}/\text{PM}_{2.5}$ Air Quality Study (CRPAQS) agency under the management of the California Air Resources Board and by the U.S. Environmental Protection Agency under Contract #R-82805701 for the Fresno Supersite.

References

- Andrews, E., P. Saxena, S. Musarra, L.M. Hildemann, P. Koutrakis, P.H. McMurry, I. Olmez, and W.H. White (2000), Concentration and composition of atmospheric aerosols from the 1995 SEAVS Experiment and a review of the closure between chemical and gravimetric measurements, *Journal of the Air and Waste Management Association*, 50(5), 648-664.
- Baldauf, R.W., D.D. Lane, G.A. Marotz, and R.W. Wiener (2001), Performance evaluation of the portable MiniVol particulate matter sampler, *Atmos. Environ.*, 35, 6087-6091.
- Barber, C.B., D.P. Dobkin, and H.T. Huhdanpaa (1996), The Quickhull Algorithm for Convex Hulls, *ACM Transactions on Mathematical Software*, 22(4), 469-483.
- Chen, L.-W.A., B.G. Doddridge, R.R. Dickerson, J.C. Chow, and R.C. Henry (2002), Origins of fine aerosol mass in the Baltimore-Washington corridor: Implications from observation, factor analysis, and ensemble air parcel back trajectories, *Atmos. Environ.*, 36(28), 4541-4554.
- Chen, L.-W.A., B.G. Doddridge, J.C. Chow, R.R. Dickerson, W.F. Ryan, and P.K. Mueller (2003), Analysis of summertime $\text{PM}_{2.5}$ and haze episode in the mid-Atlantic region, *Journal of the Air and Waste Management Association*, 53(8), 946-956.
- Chen, L.-W.A., J.C. Chow, J.G. Watson, H. Moosmüller, and W. P. Arnott (2004), Modeling reflectance and transmittance of quartz-fiber filter samples containing elemental carbon particles: Implications for thermal/optical analysis, *J. Aerosol Sci.*, 35(6), 765-780, doi: 10.1016/j.jaerosci.2003.12.005.

- Chow, J.C., and J.G. Watson (2002), PM_{2.5} carbonate concentrations at regionally representative Interagency Monitoring of Protected Visual Environment sites, *Journal of Geophysical Research*, 107(D21), ICC 6-1-ICC 6-9, doi: 10.1029/2001JD000574.
- Chow, J.C., J.G. Watson, D.H. Lowenthal, P.A. Solomon, K.L. Magliano, S.D. Ziman, and L.W. Richards (1992), PM₁₀ source apportionment in California's San Joaquin Valley, *Atmos. Environ.*, 26A(18), 3335-3354.
- Chow, J.C., J.G. Watson, D.H. Lowenthal, P.A. Solomon, K.L. Magliano, S.D. Ziman, and L.W. Richards (1993), PM₁₀ and PM_{2.5} compositions in California's San Joaquin Valley, *Aerosol Sci. Technol.*, 18,105-128.
- Chow, J.C., J.G. Watson, D.H. Lowenthal, P.A. Solomon, K.L. Magliano, S.D. Ziman, and L.W. Richards (1994), PM₁₀ and PM_{2.5} chemical characteristics and source apportionment in the San Joaquin Valley, in: *Planning and Managing Regional Air Quality, Modeling and Measurement Studies*, edited by P.A. Solomon, pp. 687-698, CRC Press, Inc, Boca Raton, FL.
- Chow, J.C., J.G. Watson, Z. Lu, D.H. Lowenthal, C.A. Frazier, P.A. Solomon, R.H. Thuillier, and K.L. Magliano, (1996), Descriptive analysis of PM_{2.5} and PM₁₀ at regionally representative locations during SJVAQS/AUSPEX, *Atmos. Environ.*, 30(12), 2079-2112.
- Chow, J.C., J.G. Watson, D.H. Lowenthal, R. Hackney, K.L. Magliano, D. Lehrman, and T.B. Smith (1998), Temporal variations of PM_{2.5}, PM₁₀, and gaseous precursors during the 1995 Integrated Monitoring Study in Central California, in: *Proceedings, PM_{2.5}: A Fine Particle Standard*, edited by J.C. Chow and P. Koutrakis, pp. 59-77, Air & Waste Management Association, Pittsburgh, PA.
- Chow, J.C., J.G. Watson, D.H. Lowenthal, R. Hackney, K.L. Magliano, D. Lehrman, and T. Smith (1999), Temporal variations of PM_{2.5}, PM₁₀, and gaseous precursors during the 1995 Integrated Monitoring Study in central California, *Journal of the Air and Waste Management Association*, 49(PM), PM16-PM24.
- Chow, J.C., J.G. Watson, D. Crow, D.H. Lowenthal, and T.M. Merrifield (2001), Comparison of IMPROVE and NIOSH carbon measurements, *Aerosol Sci. Technol.*, 34(1), 23-34.
- Chow, J.C., J.G. Watson, L.-W.A. Chen, W.P. Arnott, H. Moosmüller, and K.K. Fung (2004), Equivalence of elemental carbon by Thermal/Optical Reflectance and Transmittance with different temperature protocols, *Environ. Sci. Technol.*, 38(16), 4414-4422.
- Chow, J.C., J.G. Watson, D.H. Lowenthal, and K. Magliano (2005), Loss of PM_{2.5} nitrate from filter samples in central California, *Chemosphere*, accepted.
- Fine, P.M., G.R. Cass, and B.R.T. Simoneit (2002), Organic compounds in biomass smoke from residential wood combustion: Emissions characterization at a continental scale, *Journal of Geophysical Research*, 107(D21), ICC 11-1-ICC 11-9, doi:10.1029/2001JD000661.

- Herring S., and Cass G. (1999), The magnitude of bias in the measurement of PM_{2.5} arising from volatilization of particulate nitrate from Teflon filters, *Journal of the Air and Waste Management Association*, 49(6), 725-733.
- Khlystov, A., C.O. Stanier, S. Takahama, and S.N. Pandis (2005), Water content of ambient aerosol during the Pittsburgh air quality study. *Journal of Geophysical Research*, 110(D7).
- Magliano, K.L., A.J. Ranzieri, and P.A. Solomon (1998a), Chemical mass balance modeling of the 1995 Integrated Monitoring Study database, in: *Proceedings, PM_{2.5}: A Fine Particle Standard*, edited by J. C. Chow and P. Koutrakis, pp. 824-838, Air & Waste Management Association, Pittsburgh, PA.
- Magliano, K.L.; A.J. Ranzieri, P.A. Solomon, and J.G. Watson (1998b), Chemical mass balance modeling of data from the 1995 Integrated Monitoring Study, California Regional PM₁₀/PM_{2.5} Air Quality Study, California Air Resources Board, Sacramento, CA.
- Magliano, K.L., V.M. Hughes, L.R. Chinkin, D.L. Coe, T.L. Haste, N. Kumar, and F.W. Lurmann (1999), Spatial and temporal variations in PM₁₀ and PM_{2.5} source contributions and comparison to emissions during the 1995 Integrated Monitoring Study, *Atmos. Environ.*, 33(29), 4757-4773.
- Malm, W.C., J.F. Sisler, D. Huffman, R.A. Eldred, and T.A. Cahill (1994), Spatial and seasonal trends in particle concentration and optical extinction in the United States, *Journal of Geophysical Research*, 99(D1), 1347-1370.
- Malm, W.C., B.A. Schichtel, M.L. Pitchford, L.L. Ashbaugh, and R.A. Eldred (2004), Spatial and monthly trends in speciated fine particle concentration in the United States, *Journal of Geophysical Research*, 109(D03306), doi:10.1029/2003JD003739.
- Mochida, M., and K. Kawamura (2004), Hygroscopic properties of levoglucosan and related organic compounds characteristic to biomass burning aerosol particles, *Journal of Geophysical Research*, 109(D21202), doi:10.1029/2004JD004962.
- Rees S.L., Robinson A.L., Khlystov A., Stanier C.O., Pandis S.N. (2004), Mass balance closure and the federal reference method for PM_{2.5} in Pittsburgh, Pennsylvania, *Atmos. Environ.*, 38(20), 3305-3318.
- Sandwell, David T. (1987), Biharmonic Spline Interpolation of GEOS-3 and SEASAT Altimeter Data, *Geophysical Research Letters*, 2, 139-142.
- Schauer, J.J., and G.R. Cass (2000), Source apportionment of wintertime gas-phase and particle-phase air pollutants using organic compounds as tracers, *Environ. Sci. Technol.* 34(9), 1821-1832.
- Simoneit, B.R.T. (2002), Chemical characterization of sub-micron organic aerosols in the tropical trade winds of the Caribbean using gas chromatography-mass spectrometry, *Atmos. Environ.*, 36(33), 5259-5263.

- Simoneit, B.R.T., J.J. Schauer, C.G. Nolte, D.R. Oros, V.O. Elias, M.P. Fraser, W.F. Rogge, and G.R. Cass (1999), Levoglucosan, a tracer for cellulose in biomass burning and atmospheric particles, *Atmos. Environ.*, 33(2), 173-182.
- Smith, T.B., and D.E. Lehrman (2004), Long-range tracer studies in the San Joaquin Valley, in: *Proceedings, Regional Photochemical Measurement and Modeling Studies*, Volume 1, edited by A. J. Ranzieri and P. A. Solomon, pp. 151-165, Air & Waste Management Association, Pittsburgh, PA.
- Subramanian, R., A.Y. Khlystov, J.C. Cabada, and A.L. Robinson (2004), Positive and negative artifacts in particulate organic carbon measurements with denuded and undenuded sampler configurations, *Aerosol Sci. Technol.*, 38(Suppl 1), 27-48.
- Turpin, B.J., and H. J. Lim (2001), Species contributions to PM_{2.5} mass concentrations: Revisiting common assumptions for estimating organic mass., *Aerosol Sci. Technol.*, 35(1), 602-610.
- Turpin, B.J., J.J. Huntzicker, and S.V. Hering (1994), Investigation of organic aerosol sampling artifacts in the Los Angeles Basin, *Atmos. Environ.*, 28(19), 3061-3071.
- U.S. EPA (1997), National ambient air quality standards for particulate matter: Final rule, *Federal Register*, 62(138), 38651-38701, <http://www.epa.gov/ttn/amtic/files/cfr/recent/pmnaaqs.pdf>
- U.S.EPA (2004), Final rule to implement the 8-hour ozone national ambient air quality standard-Phase I. *Federal Register*, 69(84), 23951-24000.
- Watson, J.G. and J.C. Chow (2002), A wintertime PM_{2.5} episode at the Fresno, CA, Supersite, *Atmos. Environ.*, 36(3), 465-475.
- Watson, J.G., J.C. Chow, Z. Lu, E.M. Fujita, D.H. Lowenthal, and D.R. Lawson (1994), Chemical mass balance source apportionment of PM₁₀ during the Southern California Air Quality Study, *Aerosol Sci. Technol.*, 21(1), 1-36.
- Watson, J.G., D.W. DuBois, R. DeMandel, A.P. Kaduwela, K.L. Magliano, C. McDade, P.K. Mueller, A.J. Ranzieri, P.M. Roth, and S. Tanrikulu (1998), Field program plan for the California Regional PM_{2.5}/PM₁₀ Air Quality Study (CRPAQS), California Air Resources Board, Desert Research Institute, Reno, NV, <http://sparc2.baaqmd.gov/centralca/publications.htm>
- Zhang, X, and P.H. McMurry (1987), Theoretical analysis of evaporative losses from impactor and filter deposits, *Atmos. Environ.*, 21, 1779-1789.
- Zhang, X.Q., and P.H. McMurry (1992), Evaporative losses of fine particulate nitrates during sampling, *Atmos. Environ.*, 26A(18), 3305-3312.

Figure Captions

Figure 1. The 24-hr speciated ambient PM_{2.5} network at 5 anchor sites (denoted with *) and 35 satellite sites during CRPAQS.

Figure 2. Spatial distribution of: (a) annual PM_{2.5} concentration (1 February 2000 – 31 January 2002) during the CRPAQS. Contours are determined with 2-dimensional cubic-spline algorithm using only sites with >70% valid measurements. The stars indicate locations of the sampling sites; and (b) Geographical cross-sections A, B, C, and D chosen to show the spatial variability of PM_{2.5} mass and chemical compositions in Figure 4.

Figure 3. Time series of PM_{2.5} at selected sites during CRPAQS including: northern boundary/background site (BODG), inter-basin anchor sites (BTI, SNFH), eastern transport site (ACP), southern transport site (TEH2), regional transport anchor site (ANGI) and two urban anchor sites (FSF and BAC). Y-axis is PM_{2.5} concentration in µg/m³. Shaded areas indicate the intensive observing periods (IOPs).

Figure 4. Chemical composition and mass closure of PM_{2.5} along the geographical cross-sections A, B, and C (defined in Figure 2b) for the low (C_{low}) (February to October 2000) and high (C_{high}) PM_{2.5} periods during CRPAQS. Y-axes are ambient concentration in unit µg/m³. Sampling sites located approximately on each cross-section are noted.

Figure 5. Seasonal variation of total ammonium (NH₃ + NH₄⁺) concentration and NH₃/NH₄⁺ ratio at Fresno during CRPAQS. Note that the y-axis on the right is in logarithm scale.

Figure 6. Spatiotemporal variations of: (a) PM_{2.5} (b) NH₄NO₃ (c) OM across the four CRPAQS IOPs. The concentrations are those along the cross-section D defined in Figure 2 (essentially a combination of the upper portion of cross-section A and lower portion of B), calculated by cubic-spline algorithm using all available measurements. Horizontal dashed lines indicate the latitude of Bethel Island (BTI), Fresno (FSF), and Bakersfield (BAC) sites.

Figure 1.

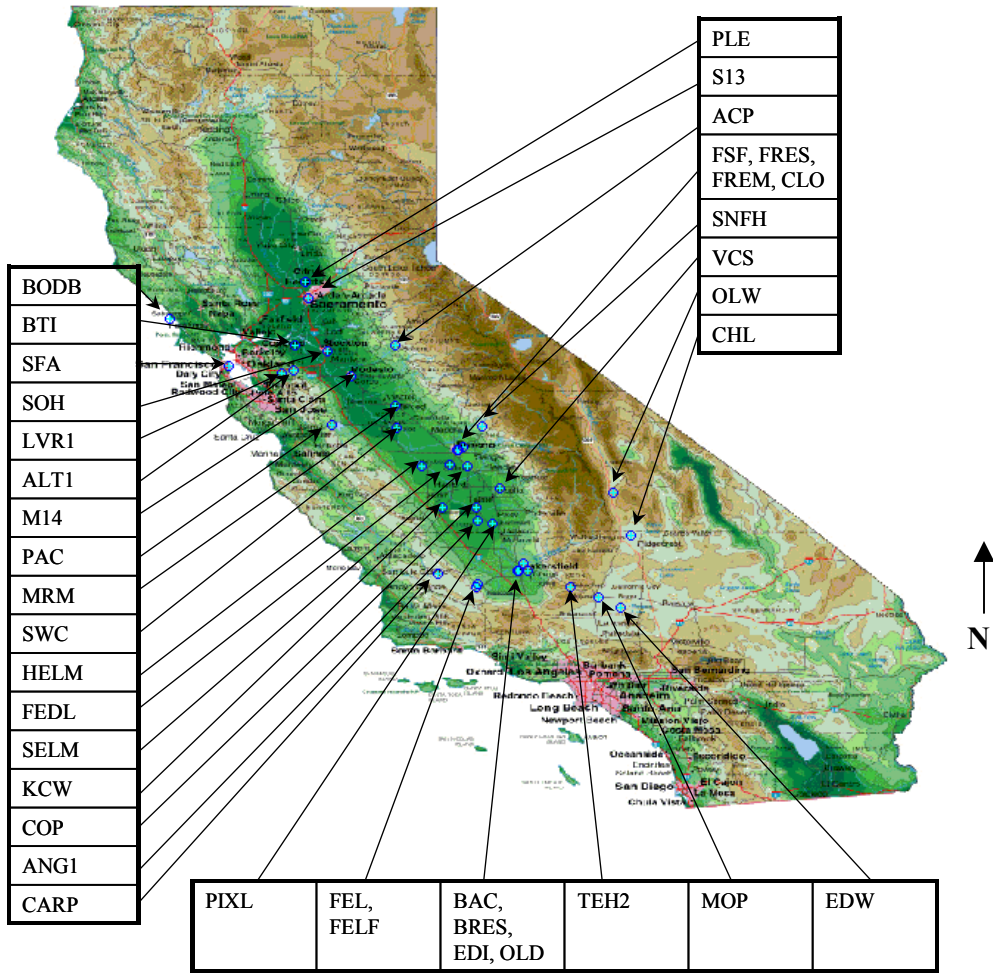
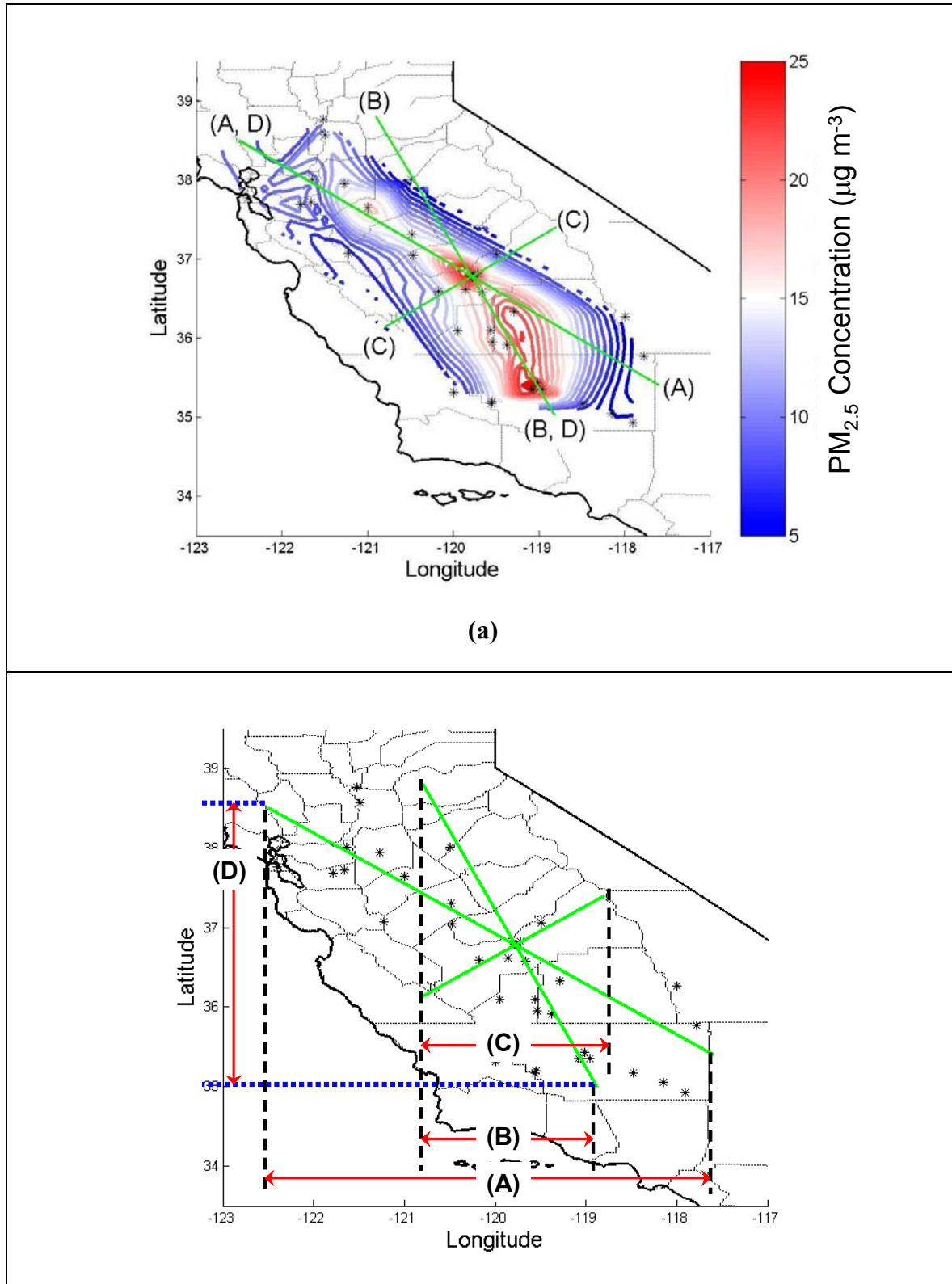


Figure 2.



(b)

Figure 3.

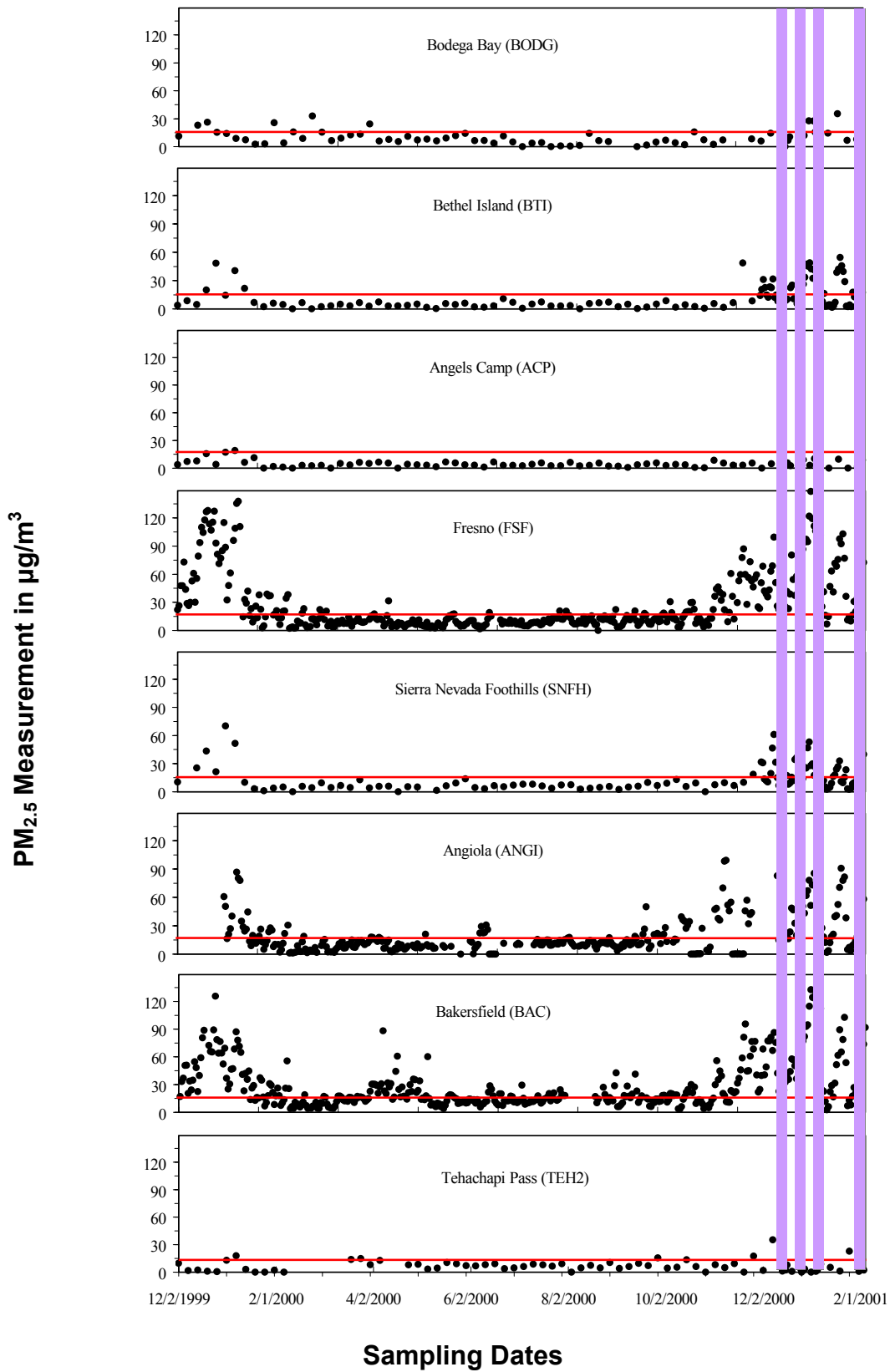
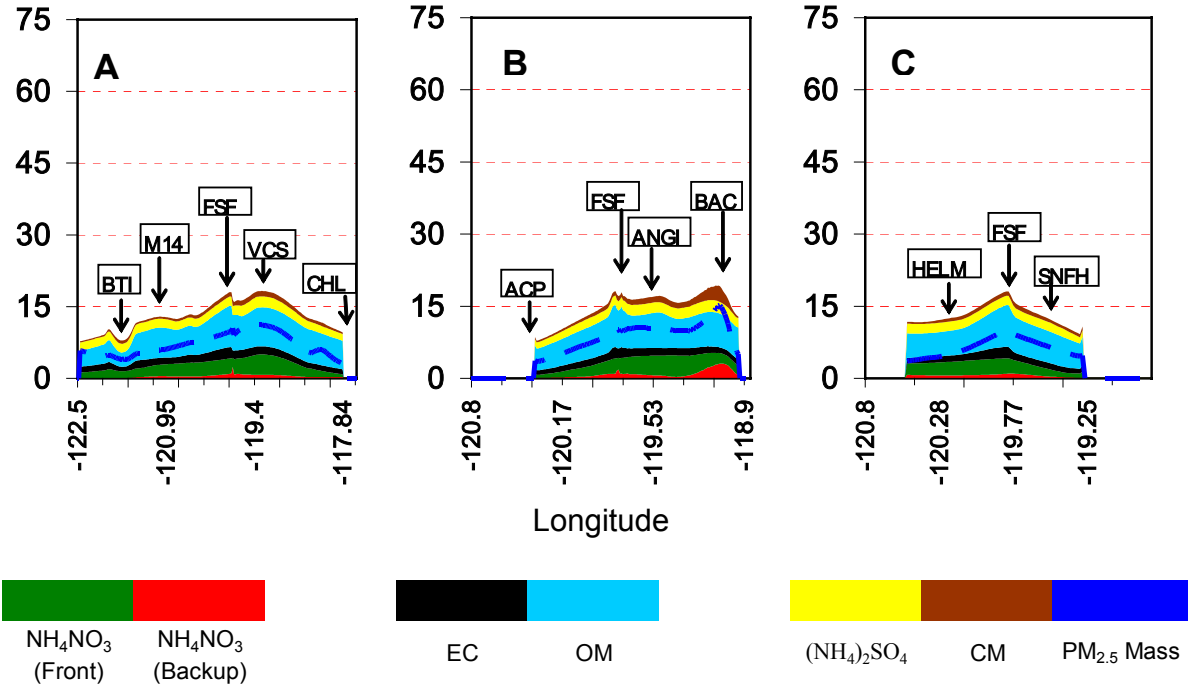


Figure 4.

Low_PM_{2.5} Period (Feb. – Oct.) Averages



High_PM_{2.5} Period (Nov. – Jan.) Averages

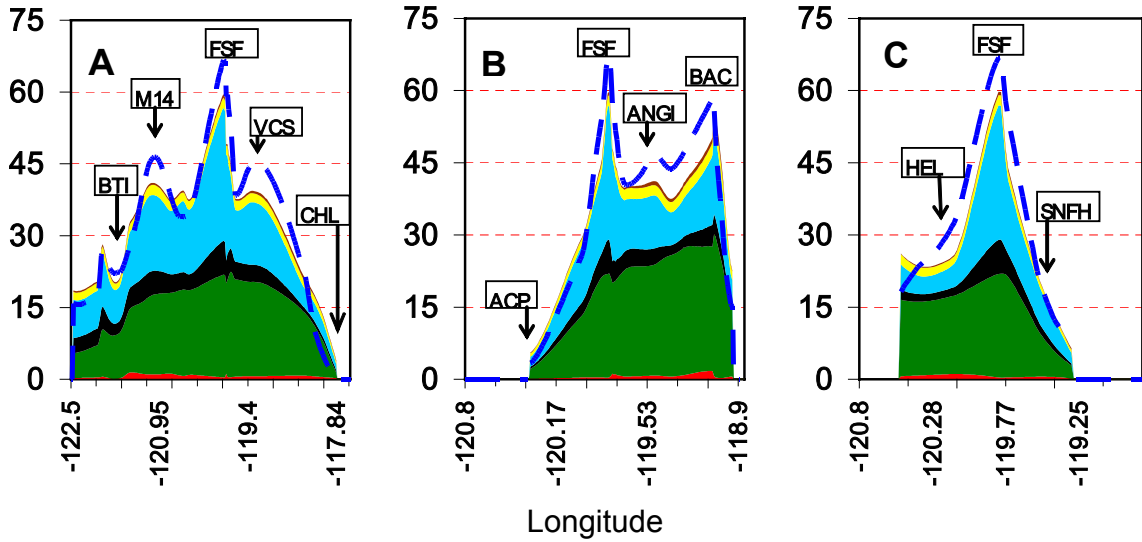


Figure 5.

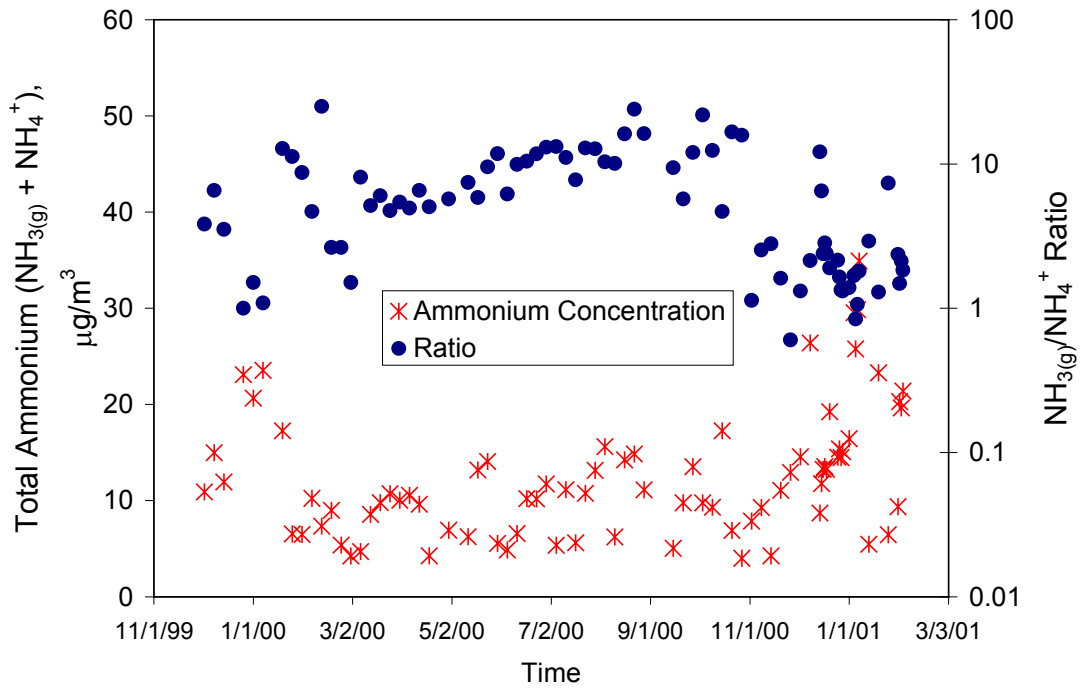


Figure 6.

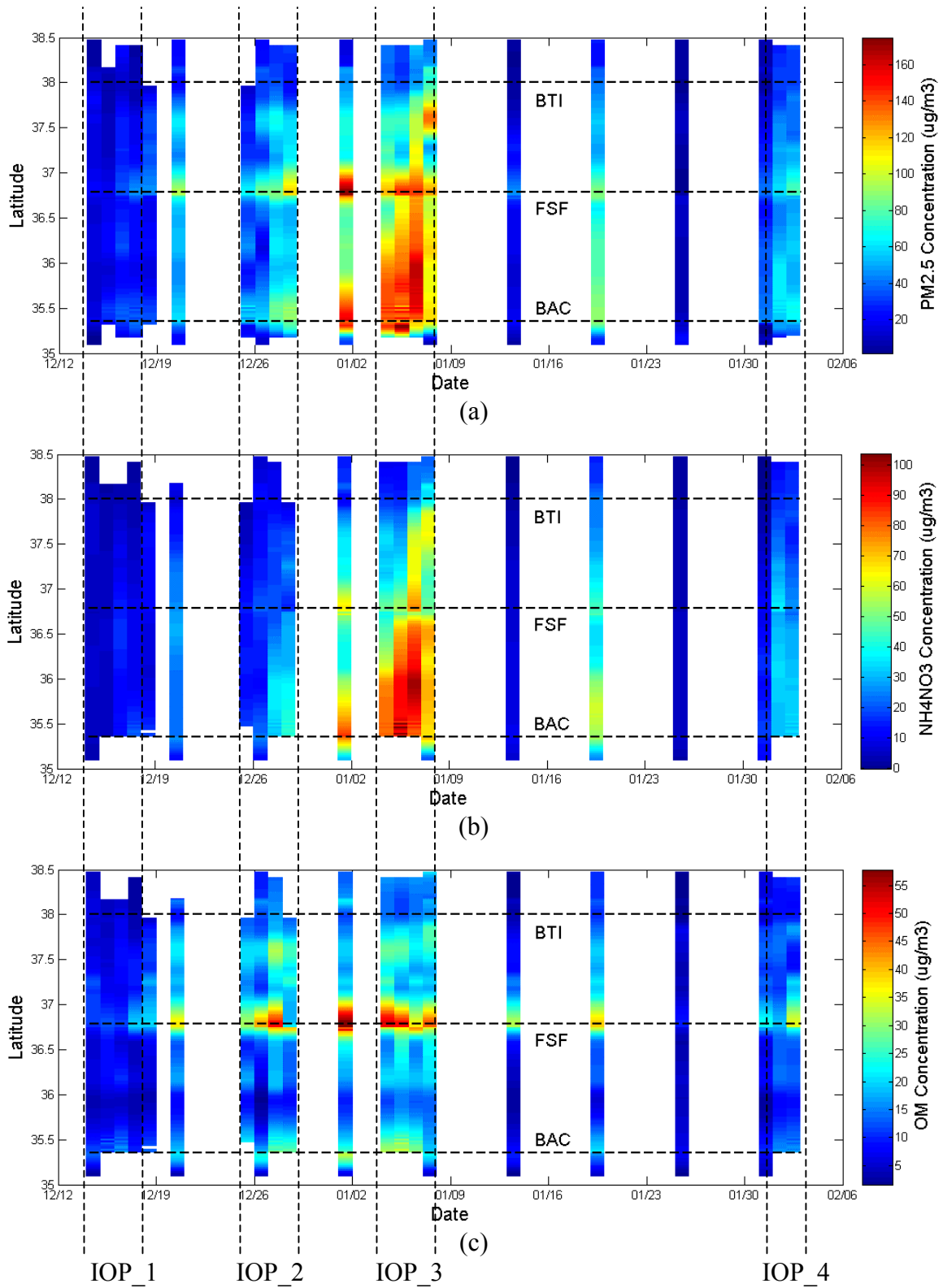


Table 1. Summary of CRPAQS aerosol measurements at the anchor and satellite sites.

Site Code	Site Name	Site Location	Site Type/Characteristics	Longitude	Latitude	Elevation (m)	Anchor Sites ^a		Satellite Sites ^b					
							Sampling Period		Filter Pack		Sampling Period		Annual	Winter Intensive
							Annual	Winter Intensive	PM _{2.5}		Annual	Winter Intensive		
									T/C	q/n			FTC ^c	FQN ^d
ACP	Angels Camp	Elevated Rural; 6850 Studhorse Flat Road, Sonora	Intrabasin Gradient	-120.491	38.006	373			FTC ^c	FQN ^d	X	X		
ALT1	Altamont Pass	Elevated rural; Flynn Road exit, I-580	Inter-basin Transport	-121.660	37.718	350			FTC		X	X		
ANGI	Angiola-ground level		Intrabasin Gradient/Transport, Vertical Gradient, Visibility	-119.538	35.948	60	X	X						
BAC	Bakersfield-5558 California Street	Rural; 36078 4th Avenue, Corcoran Urban; 5558 CA Ave. #430 (STI) #460 (ARB), Bakersfield	Community Exposure, Visibility	-119.063	35.357	119	X	X						
BODG	Bodega Marine Lab	Marine; Bodega Marine Lab, 2099 Westside Road, Bodega Bay	Boundary/Background	-123.073	38.319	17			FTC	FQN	X	X		
BRES	BAC-Residential	Urban; 7301 Remington Avenue, Bakersfield	Source- woodburning	-119.084	35.358	117			FTC	FQN	X	X		
BTI	Bethel Island	Rural; 5551 Bethel Island Road, Bethel Island	Inter-basin Transport	-121.642	38.006	2		X	FTC	FQN	X			
CARP	Carrizo Plain	Elevated rural; Soda Springs Road, 0.5 mile south of California Valley	Intrabasin Gradient, Visibility	-119.996	35.314	598			FTC		X			
CHL	China Lake	Elevated rural; Baker Site	Visibility	-117.776	35.774	684			FTC	FQN	X			
CLO	Clovis	Suburban; 908 N. Villa, Clovis	Community Exposure	-119.716	36.819	108			FTC	FQN	X	X		
COP	Corcoran-Patterson Avenue	Rural; 1520 Patterson Ave., Corcoran	Community Exposure	-119.566	36.102	63			FTC	FQN	(X) ^e	X		
EDI	Edison	Urban; 4101 Kimber Avenue, Bakersfield	Intrabasin Gradient	-118.957	35.350	118			FTC		X	X		
EDW	Edwards Air Force Base	Elevated rural; North end of Rawinsonde Road, Edwards AFB	Intrabasin Gradient, Visibility	-117.904	34.929	724			FTC	FQN	X			
FEDL	Feedlot or Dairy	Rural; 8555 S. Valentine, Fresno (near Raisin City)	Source - Cattle	-119.855	36.611	76			FTC	FQN	X	X		
FEL	Fellows	Elevated rural; Across from 25883 Hwy 33, Fellows	Source- Oilfields	-119.546	35.203	359			FTC	FQN	X	X		
FELF	Foothills above Fellows	Elevated rural; Texaco Pump Site 47-1, Fellows	Intrabasin Gradient	-119.557	35.171	512			FTC	FQN	X	X		
FREM	Fresno MV	Urban; Pole #16629, 2253 E. Shields Ave., Fresno	Source - Motor Vehicle	-119.783	36.780	96			FTC	FQN	X	X		
FRES	Residential area near FSF, with woodburning	Urban; Pole #16962, 3534 Virginia Lane, Fresno	Source - Woodburning	-119.768	36.783	97			FTC	FQN	(X)	X		
FSF	Fresno-3425 First Street	Urban; 3425 First Street, Fresno	Community Exposure, Visibility	-119.773	36.782	97	X	X						
HELM	Agricultural fields/Helm-Central Fresno County	Rural; Near Placer & Springfield	Intrabasin Gradient	-120.177	36.591	55			FTC	FQN	X	X		
KCW	Kettleman City	Rural; Omaha Avenue 2 miles west of Hwy 41, Kettleman City	Intrabasin Gradient	-119.948	36.095	69			FTC		X	X		
LVR1	Livermore - New site	Rural; 793 Rincon Street, Livermore	Inter-basin Transport	-121.784	37.688	138			FTC	FQN	X	X		
M14	Modesto 14th St.	Urban; 814 14th Street, Modesto	Community Exposure	-120.994	37.642	28			FTC	FQN	(X)	X		
MOP	Mojave-Poole	Elevated rural; 923 Poole Street, Mojave	Community Exposure	-118.148	35.051	832			FTC	FQN	X			
MRM	Merced-midtown	Suburban; 2334 M Street, Merced	Community Exposure	-120.481	37.308	53			FTC	FQN	X	X		
OLD	Oildale-Manor	Suburban; 3311 Manor Street, Oildale	Community Exposure	-119.017	35.438	180			FTC	FQN	(X)			

Table 1. Continued.

Site Code	Site Name	Site Location	Site Type/Characteristics	Longitude	Latitude	Elevation (m)	Anchor Sites ^a		Satellite Sites ^b			
							Sampling Period		Filter Pack		Sampling Period	
							Annual	Winter Intensive	PM _{2.5}		Annual	Winter Intensive
		T/C	q/n									
ACP	Angels Camp	Elevated Rural; 6850 Studhorse Flat Road, Sonora	Intrabasin Gradient	-120.491	38.006	373			FTC ^c	FQN ^d	X	X
ALT1	Altamont Pass	Elevated rural; Flynn Road exit, I-580	Inter-basin Transport	-121.660	37.718	350			FTC		X	X
ANGI	Angiola-ground level	Rural; 36078 4th Avenue, Corcoran	Intrabasin Gradient/Transport, Vertical Gradient, Visibility	-119.538	35.948	60	X	X				
OLW	Olancho	Elevated rural; Just to east of Hwy 395	Background	-117.993	36.268	1124			FTC	FQN	X	X
PAC	Pacheco Pass	Elevated rural; Upper Cottonwood Wildlife Area, west of Los Banos	Inter-basin Transport	-121.222	37.073	452			FTC		X	
PIXL	Pixley Wildlife Refuge	Rural; Road 88, 1.5 miles north of Avenue 56, Alpaugh	Rural, Intrabasin Gradient	-119.376	35.914	69			FTC	FQN	X	X
PLE	Pleasant Grove (north of Sacramento)	Rural; 7310 Pacific Avenue, Pleasant Grove	Intrabasin Gradient	-121.519	38.766	10			FTC	FQN	X	
S13	Sacramento-1309 T Street	Urban; 1309 T Street, Sacramento	Community Exposure	-121.493	38.568	6			FTC	FQN	X	X
SELM	Selma(south Fresno area gradient site)	Rural; 7225 Huntsman Avenue, Selma	Community Exposure	-119.660	36.583	94			FTC	FQN	X	X
SFA	San Francisco - Arkansas	Marine/urban; 10 Arkansas St., San Francisco	Community Exposure	-122.399	37.766	6			FTC	FQN	X	
SNFH	Sierra Nevada Foothills	Elevated rural 31955 Auberry Road, Auberry	Vertical Gradient, Intrabasin Gradient, Visibility	-119.496	37.063	589		X	FTC	FQN	X	
SOH	Stockton-Hazelton	Urban; 1601 E. Hazelton, Stockton	Intrabasin Gradient	-121.269	37.950	8			FTC	FQN	X	X
SWC	SW Chowchilla	Rural; 20513 Road 4, Chowchilla	Inter-basin Transport	-120.472	37.048	43			FTC	FQN	X	X
TEH2	Tehachapi Pass	Elevated rural; Near 19805 Dovetail Court, Tehachapi	Inter-basin Transport, Visibility	-118.482	35.168	1229			FTC		X	X
VCS	Visalia Church St.	Urban; 310 Church Street, Visalia	Community Exposure	-119.291	36.333	102			FTC	FQN	(X)	X
Total Number of Sites							3	5	35	29	35	25

^a Anchor site annual sampling program used DRI medium-volume sequential filter samplers (SFS) equipped with Bendix 240 cyclone PM_{2.5} inlets and preceding anodized aluminum nitric acid denuders. Sampling was conducted daily, 24 hours/day (midnight to midnight) from 2 December 1999 to 3 February 2001 at a flow rate of 20 L/min. Two filter packs were used for sampling: 1) each Teflon/citric acid filter pack consists of a front Teflon-membrane filter (for mass, b_{abs}, and elemental analyses) backed up by a citric-acid-impregnated cellulose-fiber filter (for ammonia), and 2) each quartz/NaCl filter pack consists of a front quartz-fiber filter (for ion and carbon analyses) backed up by a sodium-chloride-impregnated cellulose-fiber filter (for volatilized nitrate).

^b Anchor site winter intensive sampling included both SFS for PM_{2.5} sampling and sequential gas samplers (SGS) for ammonia and nitric acid sampling by denuder difference on 15 forecast episode days (15 December 2000 to 18 December 2000, 26 December 2000 to 28 December 2000, 4 January 2001 to 7 January 2001, and 31 January 2001 to 3 February 2001). The two SGS were equipped with: 1) citric-acid-coated glass denuders and quartz-fiber filters backed up by citric-acid-impregnated cellulose-fiber filters for ammonia (NH₃); and 2) anodized aluminum denuders and quartz-fiber filters backed up by sodium-chloride-impregnated cellulose-fiber filters for nitric acid (HNO₃). VOCs and carbonyls were sampled 4 times/day (0000-0500, 0500-1000, 1000-1600, and 1600-2400 PST) at 4 anchor sites (Angiola, Fresno, Bethel Island, and Sierra Foothill). Heavy hydrocarbons were sampled with Tenax and PUF/XAD samplers 4 times/day (0000-0500, 0500-1000, 1000-1600, and 1600-2400 PST) at the Fresno anchor site and 2 times/day (0500-1600 and 1600-next day 0500 PST) at the Bethel Island, Sierra Foothill, and Angiola anchor sites.

^c FTC filter pack: Teflon-membrane filter samples were analyzed for mass by gravimetry, filter light transmission (b_{abs}) by densitometry, and elements (Na, Mg, Al, Si, P, S, Cl, K, Ca, Ti, V, Cr, Mn, Fe, Co, Ni, Cu, Zn, Ga, As, Se, Br, Rb, Sr, Y, Zr, Mo, Pd, Ag, Cd, In, Sn, Sb, Ba, La, Au, Hg, Tl, Pb, and U) by x-ray fluorescence (Watson et al., 1999); quartz-fiber filter samples were analyzed for anions (chloride [Cl⁻], nitrate [NO₃⁻], sulfate [SO₄⁻]) by ion chromatography (Chow and Watson, 1999), ammonium (NH₄⁺) by automated colorimetry, water-soluble Na⁺ and K⁺ by atomic absorption

spectrophotometry, and 7-fraction organic and elemental carbon (OC1 combusted at 120 °C, OC2 at 250 °C, OC3 at 450 °C, OC4 at 550 °C, EC1 at 550 °C, EC2 at 700 °C, and EC3 at 800 °C with pyrolysis correction) by thermal/optical reflectance (Chow et al., 1993a, 2001); citric-acid-impregnated filter samples were analyzed for ammonia (NH₃) by automated colorimetry; and sodium-chloride-impregnated filters were analyzed for volatilized nitrate by ion chromatography.

^d Sampling with battery-powered Minivol samplers (Airmetrics, Eugene, OR) equipped with PM₁₀/PM_{2.5} (in tandem) or PM₁₀ inlets at a flow rate of 5 L/min.

^e (X) Includes the PM₁₀ sites operated during the annual program.

Table 2. Summary of PM_{2.5} mass and chemical composition at 38 sites during CRPAQS. (Coded in bold are anchor sites, refer Table 1 for site codes.)

Site Code	14-Month/ ^a Annual ^b Valid PM _{2.5} Measurements	Spring Mean PM _{2.5} (μg/m ³) ^c	Summer Mean PM _{2.5} (μg/m ³) ^c	Fall Mean PM _{2.5} (μg/m ³) ^c	Winter Mean PM _{2.5} (μg/m ³) ^c	Annual Means from Quarters (μg/m ³) ^d	Annual Mean PM _{2.5} (μg/m ³) ^b	14-Month Mean PM _{2.5} (μg/m ³) ^a	Maximum PM _{2.5} (μg/m ³)	Maximum Date (d/m/yyyy)	C _{high} ^g (μg/m ³) ^e	C _{low} ^g (μg/m ³) ^f	F _{high} ^g (%) ^g	Annual ^m NH ₄ NO ₃ (μg/m ³) ^h	Annual ^m OM (μg/m ³) ⁱ	Annual ^m EC (μg/m ³)	Annual ^m (NH ₄) ₂ SO ₄ (μg/m ³) ^j	Annual ^m Crustal (μg/m ³) ^k	Sumed PM _{2.5} Mass (μg/m ³) ^l	PM _{2.5} Mass Closure (%) ⁿ
ACP	72/61	3.93 ± 2.08	3.59 ± 1.62	3.56 ± 2.17	5.02 ± 5.41	3.40	3.39 ± 2.14	4.17 ± 3.62	18.94	7/1/2000	3.46	3.36	26	1.05	3.83	0.87	1.14	0.36	7.26	214
ALT1	68/61	4.16 ± 1.82	5.14 ± 2.63	6.13 ± 10.22	13.34 ± 18.66	7.25	7.31 ± 11.69	7.78 ± 12.19	71.65	7/1/2001	16.76	3.95	59	-	-	-	-	0.35	-	-
ANGI	55/50	10.85 ± 3.94	11.42 ± 5.60	20.59 ± 26.68	29.13 ± 31.02	18.68	19.12 ± 23.66	19.26 ± 23.09	123.43	7/1/2001	41.39	11.30	55	9.54	5.35	0.82	2.03	2.96	20.70	108
BAC	66/57	19.77 ± 12.79	13.30 ± 2.93	23.15 ± 22.01	43.47 ± 36.72	25.99	26.98 ± 27.50	28.08 ± 27.70	132.70	1/1/2001	56.91	15.30	55	12.13	9.88	1.96	2.63	3.43	30.02	111
BODB	67/57	10.48 ± 4.90	4.64 ± 4.10	5.49 ± 4.31	14.80 ± 9.76	8.95	9.31 ± 7.84	9.96 ± 8.07	35.34	19/1/2001	13.55	7.93	36	1.64	1.62	0.36	1.86	0.15	5.63	60
BRES	45/40	7.90 ± 3.09	7.56 ± 2.50	20.06 ± 27.55	53.58 ± 42.09	43.74	27.88 ± 36.54	30.63 ± 36.75	158.94	1/1/2001	59.06	7.10	74	11.46	9.95	2.78	2.14	1.38	27.71	99
BTI	72/61	4.06 ± 1.85	4.53 ± 2.92	6.95 ± 11.85	18.54 ± 19.19	8.81	8.88 ± 13.85	9.99 ± 14.24	76.57	7/1/2001	22.77	3.94	66	3.65	4.15	1.32	1.67	0.73	11.52	130
CARP	63/63	4.24 ± 2.34	3.40 ± 2.18	7.49 ± 8.06	8.33 ± 10.03	5.46	6.04 ± 7.05	6.24 ± 7.44	32.56	19/1/2001	11.80	3.88	50	-	-	-	-	0.86	-	-
CHL	60/51	2.09 ± 1.33	3.32 ± 2.52	1.44 ± 1.42	5.65 ± 16.40	4.72	1.90 ± 1.84	3.44 ± 9.81	74.50	7/1/2000	0.78	2.36	10	0.56	4.13	0.78	1.03	0.43	6.93	366
CLO	66/56	7.83 ± 3.41	8.64 ± 2.50	21.43 ± 30.95	47.04 ± 38.23	20.64	20.75 ± 27.78	25.32 ± 31.95	130.12	1/1/2001	55.60	9.13	67	8.56	9.63	2.46	1.88	1.21	23.74	114
COP	71/60	9.99 ± 7.02	7.96 ± 1.72	20.01 ± 19.18	37.79 ± 35.65	17.90	18.20 ± 22.60	21.86 ± 26.54	124.73	7/1/2001	42.33	9.43	60	9.32	7.16	1.71	1.98	1.62	21.80	120
EDI	64/55	10.03 ± 5.71	10.53 ± 3.34	32.24 ± 43.80	38.27 ± 40.01	24.87	24.46 ± 34.46	24.90 ± 33.19	160.83	1/1/2001	48.00	14.80	52	-	-	-	-	3.07	-	-
EDW	50/47	4.55 ± 2.08	6.25 ± 1.32	4.95 ± 4.72	5.12 ± 4.91	5.04	5.35 ± 3.58	5.27 ± 3.72	16.93	21/9/2000	5.57	5.25	26	1.89	4.02	0.84	1.50	0.79	9.05	169
FEDL	38/38	- ± -	27.77 ± 12.26	25.26 ± 15.26	38.61 ± 32.68	28.76	29.92 ± 21.31	29.92 ± 21.31	115.67	7/1/2001	38.41	23.74	35	10.83	9.66	1.87	2.30	3.36	28.01	94
FEL	71/61	7.53 ± 6.92	5.37 ± 1.49	13.42 ± 19.23	20.06 ± 20.64	12.15	12.20 ± 16.37	12.73 ± 16.37	74.16	1/1/2001	30.03	5.87	63	6.25	5.53	1.09	2.07	1.24	16.17	133
FELF	70/60	5.08 ± 2.82	4.91 ± 1.72	13.20 ± 18.13	19.57 ± 18.31	11.63	11.64 ± 15.42	11.96 ± 15.10	69.43	1/1/2001	29.53	5.13	66	7.20	5.25	0.94	2.19	0.62	16.20	139
FREM	67/60	9.66 ± 3.60	9.13 ± 2.93	21.80 ± 27.21	56.45 ± 47.69	24.76	25.27 ± 35.22	27.62 ± 36.35	175.99	1/1/2001	67.61	9.88	70	8.93	13.90	3.68	2.02	1.17	29.70	118
FRES	66/57	9.03 ± 3.92	7.81 ± 2.70	21.16 ± 26.97	55.92 ± 46.46	22.85	24.18 ± 33.93	28.19 ± 37.03	169.40	1/1/2001	63.32	8.90	70	8.35	11.72	2.93	1.93	0.82	25.74	106
FSF	71/60	11.23 ± 6.05	9.41 ± 2.95	20.15 ± 21.92	53.88 ± 41.51	23.31	23.73 ± 29.43	28.37 ± 33.41	148.33	1/1/2001	59.96	10.56	65	7.87	10.42	1.97	1.84	1.48	23.59	99
HELM	70/59	4.96 ± 2.00	5.53 ± 2.14	12.71 ± 15.55	25.94 ± 28.54	11.76	11.77 ± 16.28	14.42 ± 20.73	114.76	24/12/1999	30.83	5.27	66	7.20	5.01	1.45	1.81	0.82	16.29	138
KCW	64/55	6.09 ± 3.34	6.11 ± 2.22	13.88 ± 26.74	32.64 ± 32.68	40.95	12.86 ± 19.25	16.80 ± 25.25	112.66	7/1/2000	29.87	5.88	63	-	-	-	-	0.91	-	-
LVR1	72/61	6.25 ± 4.10	5.99 ± 3.64	8.67 ± 11.10	20.57 ± 22.28	10.51	10.61 ± 14.88	11.87 ± 15.80	95.42	7/1/2001	24.72	5.60	60	3.49	6.17	2.39	1.56	0.28	13.89	131
M14	71/60	6.07 ± 2.19	7.07 ± 5.07	15.98 ± 22.68	41.90 ± 34.37	17.27	17.27 ± 25.55	20.99 ± 27.71	136.07	7/1/2001	47.82	6.16	72	6.77	9.15	2.40	1.96	0.61	20.90	121
MOP	69/58	5.55 ± 3.62	5.34 ± 1.95	4.79 ± 3.83	2.84 ± 3.35	4.43	4.34 ± 3.25	4.36 ± 3.41	15.62	14/11/2000	2.89	4.85	17	1.45	5.01	1.11	1.39	0.62	9.58	221
MRM	72/61	6.97 ± 3.52	6.77 ± 3.33	13.03 ± 13.22	36.58 ± 28.34	13.88	14.00 ± 14.42	18.88 ± 22.52	115.87	20/12/1999	32.45	7.43	59	6.85	8.89	2.20	1.76	0.71	20.40	146
OLD	65/55	9.55 ± 5.65	7.65 ± 1.99	23.07 ± 26.78	40.91 ± 38.45	21.51	21.08 ± 28.99	23.46 ± 29.90	140.63	1/1/2001	52.58	8.15	68	11.99	8.96	1.86	2.56	1.33	26.70	127
OLW	65/54	3.09 ± 4.35	5.47 ± 9.89	1.52 ± 1.33	2.96 ± 3.91	3.21	3.13 ± 5.85	3.24 ± 5.60	39.21	27/7/2000	1.95	3.58	15	0.37	4.01	0.68	0.84	0.74	6.64	212
PAC	71/61	3.47 ± 2.11	2.91 ± 1.64	4.65 ± 8.27	14.22 ± 17.61	6.06	6.11 ± 9.23	7.38 ± 12.15	64.32	24/12/1999	15.00	2.94	63	-	-	-	-	0.13	-	-
PIXL	69/61	9.79 ± 6.70	10.04 ± 8.16	17.70 ± 14.49	38.56 ± 33.05	18.36	18.47 ± 21.54	21.16 ± 24.14	106.56	7/1/2001	42.90	9.78	59	10.32	6.01	1.62	2.16	1.32	21.44	116
PLE	70/59	6.44 ± 2.47	6.43 ± 2.55	9.06 ± 9.75	17.95 ± 17.99	9.11	9.14 ± 9.07	11.11 ± 12.72	66.30	20/12/1999	18.59	5.63	52	3.16	6.76	1.87	1.44	0.52	13.76	150

Table 2. Continued

Site Code	14-Month ^a / Annual ^b Valid PM _{2.5} Measurements	Spring Mean PM _{2.5} (µg/m ³) ^c	Summer Mean PM _{2.5} (µg/m ³) ^c	Fall Mean PM _{2.5} (µg/m ³) ^c	Winter Mean PM _{2.5} (µg/m ³) ^c	Annual Means from Quarters (µg/m ³) ^d	Annual Mean PM _{2.5} (µg/m ³) ^b	14-Month Mean PM _{2.5} (µg/m ³) ^a	Maximum PM _{2.5} (µg/m ³)	Maximum Date	C _{high} ^e (µg/m ³) ^c	C _{low} ^f (µg/m ³) ^c	F _{high} ^g (%) ^c	Annual ^m NH ₄ NO ₃ (µg/m ³) ^h	Annual ^m OM (µg/m ³) ⁱ	Annual ^m EC (µg/m ³)	Annual ^m (NH ₄) ₂ SO ₄ (µg/m ³) ^j	Annual ^m Crustal Material (µg/m ³) ^k	Sumed PM _{2.5} Mass (µg/m ³) ^l	PM _{2.5} Mass Closure (%) ⁿ
SI3	68/58	4.50 ± 1.65	4.85 ± 2.76	10.30 ± 10.79	24.39 ± 24.02	10.88	11.10 ± 14.79	13.17 ± 17.66	90.19	20/12/1999	27.82	4.73	66	3.97	7.22	2.33	1.55	0.65	15.71	142
SELM	71/61	11.40 ± 7.34	8.90 ± 3.28	18.03 ± 16.47	41.19 ± 34.67	18.18	18.33 ± 19.43	22.76 ± 26.02	110.35	24/12/1999	40.31	10.52	56	9.10	7.81	2.26	2.22	1.14	22.54	123
SFA	72/61	7.99 ± 4.66	5.12 ± 3.72	8.96 ± 7.90	16.15 ± 14.72	9.16	9.19 ± 8.55	10.54 ± 10.75	63.36	24/12/1999	18.27	5.96	51	3.20	4.47	1.83	1.97	0.50	11.98	130
SNFH	70/60	6.32 ± 3.73	5.58 ± 1.77	7.95 ± 4.39	18.14 ± 18.57	8.46	8.52 ± 8.10	10.74 ± 12.60	70.21	1/1/2000	15.65	5.92	47	3.13	6.41	1.32	1.59	0.64	13.08	154
SOH	70/59	5.43 ± 2.33	7.22 ± 5.24	9.37 ± 9.02	31.09 ± 27.28	12.66	12.78 ± 16.51	16.11 ± 20.68	103.25	20/12/1999	32.80	5.96	65	5.47	7.22	2.22	1.91	0.62	17.45	137
SWC	70/59	7.42 ± 2.51	6.45 ± 2.19	13.69 ± 15.52	27.97 ± 28.74	13.12	12.87 ± 15.72	16.01 ± 20.86	97.41	24/12/1999	32.47	6.77	62	7.08	4.53	1.43	1.58	0.84	15.46	120
TEH2	64/53	9.12 ± 3.69	6.52 ± 2.66	7.42 ± 5.06	5.58 ± 8.94	7.25	7.30 ± 6.24	6.84 ± 6.24	35.38	8/12/2000	7.32	7.29	25	-	-	-	-	0.55	-	-
VCS	72/61	14.14 ± 8.74	9.47 ± 3.31	18.55 ± 18.06	46.88 ± 37.23	21.71	21.91 ± 24.71	25.91 ± 28.83	123.65	1/1/2001	50.30	11.82	59	10.30	9.83	2.36	2.32	1.32	26.13	119

^a Consists of 72 every-sixth-day sampling from 2 December 1999 to 3 February 2001

^b Consists of 61 every-sixth-day sampling from 1 February 2001 to 31 January 2001 (CRPAQS annual program)

^c Seasonal averages of spring (March to May), summer (June to August), fall (September to November), and winter (December to February) for the CRPAQS annual program

^d Arithmetic means of the four calendar quarters: Jan. to Mar., Apr. to Jun., Jul. to Sep., and Oct. to Dec. during the CRPAQS annual program. January is from 2001 and the rest of the months are from 2000. Strikethrough indicates <75% coverage in at least one quarter, which is not to be included in the annual average calculation based on U.S. EPA (1997)

^e Average of high PM_{2.5} period (1 November 2000 to 31 January 2001)

^f Average of low PM_{2.5} period (1 February 2000 to 31 October 2000)

^g $F_{high} = [C_{high}/C_{high}/(C_{high} + 3 \times C_{low})] \times 100\%$

^h $1.29 \times ([NO_3]_{FRONT} + [NO_3]_{BACKUP})$

ⁱ $1.4 \times [OC]$

^j $1.38 \times [SO_4^{2-}]$

^k $2.2 \times [Al] + 2.49 \times [Si] + 1.63 \times [Ca] + 2.42 \times [Fe] + 1.94 \times [Ti]$

^l $NH_4NO_3 + OM + EC + (NH_4)_2SO_4 + \text{Crustal Material}$

^m Every-sixth-day annual average

ⁿ $(\text{Summed PM}_{2.5} \text{ Mass}/\text{Every-sixth-day Annual Mean PM}_{2.5}) \times 100\%$

Table 3. Zone of representations for 26 non-boundary sites inside the San Joaquin Valley on different temporal scales in kilometers. (Sites are arranged from north to south; anchor sites are noted in bold.)

Site Code	Annual			(C _{high})			(C _{low})			Episode (7 Jan 2001)		
	PM _{2.5}	NH ₄ NO ₃	OM	High_PM _{2.5} (Nov. - Jan.)	High_PM _{2.5} (Nov. - Jan.)	High_PM _{2.5} (Nov. - Jan.)	Low_PM _{2.5} (Feb. - Oct.)	Low_PM _{2.5} (Feb. - Oct.)	Low_PM _{2.5} (Feb. - Oct.)	PM _{2.5}	NH ₄ NO ₃	OM
S13	11.9	11.7	15.3	9.8	11.0	15.0	53.9	31.0	19.1	9.6	10.3	4.3
BTI	14.9	12.6	10.2	14.2	10.3	11.1	14.5	15.9	9.0	19.0	9.5	10.6
ACP	1.5	1.5	1.4	0.8	1.5	1.0	2.1	1.5	1.6	1.0	0.8	0.8
SOH	21.0	20.4	16.5	18.0	18.2	17.6	18.4	20.7	15.0	16.8	17.2	13.6
LVR1	6.3	14.9	19.7	6.1	11.5	18.2	6.7	20.7	18.6	7.8	14.3	12.3
M14	21.6	20.1	20.0	19.3	20.2	17.9	24.6	19.8	23.3	15.5	18.0	11.7
MRM	19.0	14.3	11.5	15.2	14.2	10.7	27.3	15.5	12.8	5.9	11.6	10.8
SNFH	6.1	4.5	13.6	4.0	4.3	6.5	11.5	5.0	25.8	1.5	0.9	2.8
SWC	12.8	34.1	5.7	12.7	25.1	3.1	14.6	37.7	9.1	11.9	20.9	3.6
CLO	5.6	10.1	3.2	5.8	9.5	2.6	19.2	11.2	31.2	3.0	4.0	2.6
FRES	9.5	17.1	6.4	7.5	17.0	2.5	24.4	15.5	24.0	5.3	5.3	3.3
FSF	10.8	19.5	0.7	9.5	18.2	2.2	13.5	11.7	0.8	1.9	2.9	2.4
FREM	8.5	16.3	3.0	4.5	16.2	0.9	17.9	13.8	14.8	0.8	6.2	0.9
HELM	9.6	27.2	8.9	9.2	27.6	4.9	10.5	28.3	16.3	12.4	21.6	4.6
SELM	13.6	21.4	8.7	11.9	18.9	8.4	19.5	22.7	16.6	13.3	10.0	10.0
VCS	23.1	19.1	24.5	20.7	18.0	21.1	28.1	21.1	31.5	13.6	8.7	18.2
COP	21.8	22.8	7.3	21.4	27.2	7.7	16.7	16.2	7.2	19.2	18.3	7.5
KCW	16.1	-	-	16.1	-	-	11.0	-	-	10.9	-	-
ANGI	18.6	19.3	8.2	18.7	19.0	12.2	15.9	15.7	6.8	16.6	13.7	11.1
PIXL	14.9	25.2	8.4	13.0	28.7	5.9	30.5	18.0	10.6	33.0	17.2	8.9
CHL	5.3	13.6	19.4	2.2	12.6	4.8	7.1	3.9	49.1	5.0	15.0	8.7
OLD	5.9	20.8	27.3	15.0	11.3	4.0	2.9	5.5	25.3	14.3	18.1	5.5
BAC	6.8	11.9	13.9	4.4	3.4	3.0	4.8	7.9	44.5	6.6	7.9	3.2
EDI	5.6	-	-	6.8	-	-	4.0	-	-	5.7	-	-
FEL	9.5	2.6	14.1	10.6	9.5	4.5	7.3	2.0	49.0	1.6	1.6	1.8
MOP	8.2	3.1	19.4	3.2	1.6	2.9	15.0	7.7	52.0	3.1	0.8	2.3